Results in Engineering 31 (2026) 111529

Contents lists available at ScienceDirect

Results in Engineering

journal homepage: www.sciencedirect.com/journal/results-in-engineering

Research paper

Industrial upscaling of waste mineral wool valorisation in the circular economy perspective: Integrating secondary and local raw materials in the European ceramic industry

Sonia Conte [a], Francesco Colombo [b], Mattia Sisti [b], Riccardo Fantini [b], Andrea Bresciani [c], Marco Gaddoni [c], Alessandro Francini [d], Antonella Sola [d], Annamaria Ferrari [d], Martina Napolitano [e], Alessandro F. Gualtieri [b], Rossella Arletti [b,*]

[a] CNR-ISSMC, National Research Council, Institute of Science, Technology and Sustainability for Ceramics, Via Granarolo 64, 48018, Faenza, Italy
[b] Department of Chemical and Geological Sciences – University of Modena and Reggio Emilia, Via G. Campi, 103, 41125, Modena, Italy
[c] SACMI Group, Italy
[d] Department of Sciences and Methods for Engineering, University of Modena and Reggio Emilia, Via Amendola 2, 42122, Reggio Emilia, Italy
[e] Department of Engineering Enzo Ferrari – University of Modena and Reggio Emilia, Via P. Vivarelli, 6, 41125, Modena, Italy

ARTICLE INFO

Keywords:
Scale up
Secondary raw materials
TRL6
Ceramic

ABSTRACT

The transition toward a circular economy requires the ceramic industry to reduce dependence on primary raw materials and integrate secondary resources into established production routes. In this study, the valorisation of waste mineral wool, previously transformed through thermal inertization into a homogeneous glass (named Re.Wo), is scaled up from laboratory validation to pilot-plant production of porcelain stoneware tiles. Unlike previous investigations based on non-European raw materials and laboratory-scale tests, this work employs locally sourced European clays and sands, strengthening supply-chain resilience and environmental coherence. Four formulations were designed, including a benchmark and batches containing 2–6 wt.% Re.Wo as partial replacement of feldspar. After laboratory simulation (TRL 4), selected compositions were processed at pilot scale (TRL 6) using standard ceramic equipment under representative processing conditions for milling, spray drying, pressing, and roller-kiln firing, culminating in the production of a batch of 60 m^2 of tiles. Technological properties of unfired and fired bodies, gresification behaviour, phase evolution, and thermal stability were systematically evaluated. The successful pilot-plant production demonstrates the technical feasibility of the process, showing that Re.Wo-bearing formulations up to 4 wt.% can be processed at TRL6 while maintaining technological and mechanical performance comparable to that of the benchmark. A preliminary life cycle assessment (LCA) was conducted to evaluate the environmental implications of Re.Wo incorporation within a prospective industrial scenario. This work provides a pilot-scale proof of feasibility for the integration of inertized hazardous waste into high-value ceramic products, contributing simultaneously to landfill diversion and reduction of critical raw material use.

1. Introduction

The transition towards a circular economy is driving high-throughput industries such as ceramics and glass to reduce their dependence on primary mineral resources and to increase the use of secondary raw materials. In the porcelain stoneware sector, this need is particularly relevant because the traditional raw material portfolio—plastic clays, feldspar fluxes and silica sands—is increasingly affected by supply risks and geopolitical uncertainty [1–3]. At the same time, large volumes of silicate-based wastes and by-products generated by construction, energy production, metallurgy and other sectors are still landfilled or down-cycled, despite their chemical compatibility with ceramic and glass technologies. Their upgrading into high-value products therefore represents a promising route to improve resource efficiency, reduce environmental impacts and decrease the dependence of ceramic manufacture on virgin raw materials. Among the available

* Corresponding author.
E-mail address: rossella.arletti@unimore.it (R. Arletti).

https://doi.org/10.1016/j.rineng.2026.111529
Received 12 May 2026; Received in revised form 10 June 2026; Accepted 11 June 2026
Available online 13 June 2026
2590-1230/© 2026 The Author(s). Published by Elsevier B.V. This is an open access article under the CC BY-NC-ND license (http://creativecommons.org/licenses/by-nc-nd/4.0/).

strategies for inorganic waste valorisation, vitrification is one of the most robust for chemically complex or hazardous residues, since it converts heterogeneous wastes into homogeneous glasses in which toxic elements are immobilised and leaching is significantly reduced [4–5]. These waste-derived glasses can then be further exploited in different ways, for example as precursors for glass-ceramics or cellular glass-based materials, confirming that vitrification is not only an effective inertisation route, but also a versatile materials-design platform [5–13].

For ceramic manufacturing, however, the most direct industrial opportunity often lies not in developing entirely new glass-based products, but in using such vitrified wastes as secondary raw materials in conventional ceramic bodies. This strategy is especially attractive in the tile sector, where wet milling, spray drying, pressing and fast firing are already highly optimised and where vitreous components play a key role in sintering [e.g. 14–16]. Numerous studies have shown that different waste glasses, including soda-lime cullet, CRT glass and LCD glass, can partially replace feldspathic fluxes in porcelain stoneware and other whiteware bodies, generally lowering the optimum firing temperature [17–30].

Other studies have gone further, shifting from the use of waste-derived glasses as simple additives to their deliberate design as ceramic fluxes [31–33]. In particular, these works introduced the concept of glass-ceramic stoneware, in which feldspar was fully replaced by glasses obtained from the vitrification of different kinds of waste. Such glasses promoted the formation of crystalline phases during sintering, enabling the production of high-strength tiles [31,32]. The same research line also developed tailor-made glasses produced from mixtures of industrial wastes and glass scrap, specifically designed as alternative fluxes for porcelain stoneware formulations, demonstrating their laboratory-scale feasibility at additions of up to 7 wt.% [33].

From an industrial perspective, however, the adoption of waste-derived glasses as secondary raw materials in porcelain stoneware requires more than compliance with the technological requirements of the final product. It also demands compositional stability, reproducible fusibility and full compatibility with the production line, including grinding, slurry preparation, spray drying, pressing and fast firing [34]. In this respect, vitrified *extramuros* wastes—i.e. wastes generated outside the ceramic production line—are particularly interesting, because vitrification transforms heterogeneous and often hazardous streams into homogeneous glasses that can (i) comply with leaching and regulatory requirements, (ii) be crushed and milled using conventional ceramic equipment, and (iii) be dosed and handled in a way comparable to standard ceramic raw materials [35].

Within this framework, our group previously developed a thermal inertization process for hazardous waste mineral wool, producing a homogeneous and fibre-free glass named Re.Wo [35]. Re.Wo complies with leaching and REACH requirements and can therefore be regarded as a secondary raw material. Previous laboratory-scale studies showed that additions of 3–9 wt.% Re.Wo as a partial replacement for Na-feldspar in porcelain stoneware bodies are technologically feasible, preserving unfired and fired properties within industrially acceptable limits while lowering the optimum firing temperature [35,36]. Related investigations also confirmed the effectiveness of inertized man-made vitreous fibres in glazes and ceramic coatings [37]. This approach offered a dual benefit, combining hazardous-waste diversion from landfill with the partial substitution of non-renewable natural raw materials. However, the original porcelain stoneware study relied on Ukrainian ball clays, i.e. non-European raw materials that reduced the overall sustainability of the formulation and are currently unavailable in significant quantities because of the ongoing conflict with Russia. Moreover, that study was limited to laboratory-scale experiments and did not address the industrial replicability of the process.

More generally, although the extensive literature on waste glass and waste-derived glasses has already demonstrated their potential as secondary raw materials for ceramic products, most studies remain confined to laboratory-scale investigations, with small demonstrators [6,7,10,32,33,35]. Recent broader perspectives on ceramic recycling also highlight that, despite the growing body of literature on recycling routes, closed-loop implementation and significant scale-up remain limited in many ceramic sectors, mainly because of persistent technical, economic and regulatory barriers [38]. Systematic evidence on their robustness under realistic tile-manufacturing conditions at pilot scale is still limited [34]. Therefore, the research gap addressed in the present work is not the general feasibility of using waste-derived glasses as fluxes in porcelain stoneware, which is already well established, but the lack of systematic pilot-scale validation for vitrified hazardous waste streams under representative processing routes. In particular, it remains unclear whether the technological trends observed at laboratory scale can be reproduced under pilot-line conditions including milling, slurry preparation, spray drying, pressing and roller-kiln firing.

The present study addresses this gap by scaling up to pilot scale the use of Re.Wo in porcelain stoneware bodies previously validated at laboratory scale, with the aim of assessing their technological behaviour under conditions representative of industrial practice. A further innovative aspect lies in the adoption of a predominantly European raw-material set, replacing the extra-European clays used in the previous study. This choice improves supply-chain resilience and reduces transport-related impacts, while making the overall valorisation route more consistent with circular-economy and decarbonisation strategies. To complement the technological scale-up, a prospective Life Cycle Assessment (LCA) was also carried out, not as the main outcome of the work, but as a supporting analysis to contextualize the possible environmental implications of future industrial implementation. Overall, the proposed approach provides a pilot-scale validation of technologically feasible and environmentally motivated resource valorisation within porcelain stoneware manufacturing.

2. Materials and methods

2.1. Batch formulation and analyses

The raw materials used in this study are listed in Table 1, while their chemical and mineralogical compositions are reported in Tables 2 and 3, respectively. Details of the trace-element composition are provided in Table S1 of the Supplementary Materials. All raw materials were sourced from Italy and Germany, with the sole exception of the feldspar supplied from Turkey, which is the raw material intended to be partially replaced by Re.Wo.

Chemical characterisation of the raw materials employed was carried out by wavelength-dispersive X-ray fluorescence spectrometry (WDXRF). Measurements were performed using a PANalytical Zetium spectrometer equipped with a Rh tube anode and 4 kV X-ray generator and a WDS Zetium detector. Both major and minor elements were evaluated. Aluminium supported tab were realized mixing 2.7 g of grinded sample and 0.27 g of wax on a boric acid bed. The powders were then compressed under 15 N. Data analysis was done using calibration curves based on 60 certified silicate reference materials (list available in Table 1S of Supplementary Materials). Analyses are considered accurate within 2–5 wt% (relative) and the precision is estimated on the second decimal place.

Table 1
Summary of the raw materials employed for the project.

Name	Provenance
Clay 1	mixture from Germany and Piedmont (Italy)
Clay 2	Germany
Bentonite	Sardinia (Italy)
Feldspar	Turkey
Quartz sand	Sardinia (Italy)
Re.Wo	Glass from the inertization of hazardous mineral wool

Table 2
Chemical analyses of major and minor elements of the raw materials obtained by WDS-XRF.

Sample	SiO_2	Al_2O_3	Fe_2O_3	MnO	MgO	CaO	Na_2O	K_2O	TiO_2	P_2O_5	LOI
	(wt.%)	*(wt.%)*	*(wt.%)*	*(wt.%)*	*(wt.%)*	*(wt.%)*	*(wt.%)*	*(wt.%)*	*(wt.%)*	*(wt.%)*	*(wt.%)*
Clay 1	55.71	28.04	2.28	0.02	0.71	0.28	0.31	2.27	1.06	0.04	9.02
Clay 2	56.19	28.31	2.15	0.01	0.44	0.34	0.11	1.6	1.16	0.06	9.39
Bentonite	68.47	12.83	1.13	0.04	2.68	1.29	0.28	1.97	0.12	0.03	11.01
Feldspar	67.44	17.53	0.69	0.01	2.41	0.86	8.66	0.68	0.55	0.26	0.74
Quartz sand	73.01	13.9	0.33	0.01	0.21	4.43	0.26	4.65	0.04	0.1	2.94
Re.Wo	49.64	8.29	13.03	0.18	6.71	13.68	5.23	0.87	1.3	0.35	-

Table 3
Mineralogical composition of the raw materials (with ± errors) obtained after Rietveld refinement and refinement agreement indices (indices ($R_p = \frac{\sum |Io - Ic|}{\sum Io}$; $R_{wp} = \left[\frac{\sum w(Io - Ic)^2}{\sum wIo^2}\right]^{1/2}$; $\chi^2 = \frac{\sum w(Io - Ic)^2}{N_{obs} - N_{var}}$).

	Clay-1	Clay-2	Bentonite	Feldspar	Quartz sand
Rietveld agreement indices					
R_p (%)	6.41	7.37	5.26	9.6	7.37
R_{wp} (%)	7.81	8.75	6.62	14.57	8.16
χ^2	3.33	4.24	2.66	9.9	2.73
Phase (wt.%)					
quartz	22.0 ± 0.2	29.6 ± 0.2	10.6 ± 0.2	12.0 ± 0.2	62.0 ± 0.2
K-feldspar	6.1 ± 0.2	3.3 ± 0.2	4.9 ± 0.2	2.8 ± 0.3	25.9 ± 0.3
plagioclase	2.0 ± 0.1	-	4.2 ± 0.2	77.1 ± 0.4	1.2 ± 0.2
kaolinite	46.4 ± 0.4	52.6 ± 0.5	-	-	4.3 ± 0.3
mica/illite	3.5 ± 0.1	7.7 ± 0.2	5.6 ± 0.3	3.9 ± 0.3	0.7 ± 0.1
Ca-smectite	8.4 ± 0.4	5.8 ± 0.6	44.4 ± 0.7	-	2.5 ± 0.3
IS mixed layer clay	10.2 ± 0.3	-	13.7 ± 0.4	-	-
chlorite	-	-	-	2.2 ± 0.1	-
talc	-	-	-	0.7 ± 0.2	-
calcite	-	-	0.2 ± 0	-	3.4 ± 0.1
rutile	0.5 ± 0.1	0.3 ± 0.1	-	-	-
anatase	0.9 ± 0.1	0.8 ± 0.1	-	0.4 ± 0.1	-
clinoptilolite	-	-	1.6 ± 0.1	-	-
laumontite	-	-	-	0.9 ± 0.2	-
amorphous phase	-	-	14.8 ± 0.9	-	-
Total	100	100	100	100	100

Quantitative phase analyses (QPA) of the raw materials and of the fired samples were carried out exploiting a θ–θ Bragg-Brentano X'Pert PRO diffractometer equipped with a real time multiple strip (RTMS) detector with a Ni filtered CuKα radiation produced at 40 kV, 30 mA. The powders were mixed with 10 wt.% of corundum (Al_2O_3) as an internal standard for the determination of the amorphous phase (glass here). To avoid preferred orientation side loading of the sample powder was chosen. Data were collected in the 3–85 °2θ range using step scan of 0.0167 °2θ and a counting rate of 100 s/step ½ divergence and anti-scatter slits were used along with 15 mm beam mask and 0.02° rad Soller slits were used. Quantitative phase analyses (QPA) of all the raw materials were obtained after Rietveld refinement [39] exploiting PROFEX [40] software v. 5.3.0, while data of the fired sample at maximum densification temperature using GSAS software [41] with EXPGUI interface [42].

Four porcelain stoneware formulations were developed (Table 4): a benchmark batch (BNK), representative of a hypothetical industrial composition prepared using short-supply-chain raw materials, and three batches containing increasing amounts of Re.Wo: 2 wt.% (REWO2), 4 wt.% (REWO4) and 6 wt.% (REWO6). The chemical composition of the batches, as calculated from the chemical composition of raw materials and their percentages is reported in Table 2S. The upper limit of Re.Wo incorporation was defined on the basis of the results of our previous studies [35,36] and of literature reports on the incorporation of glassy materials into porcelain stoneware bodies [e.g. 28,43–47].

Table 4
Formulations of the batches.

Raw material	BNK	REWO2	REWO4	REWO6
Clay 1	20	20	20	20
Clay 2	18	18	18	18
Bentonite	2	2	2	2
Feldspar	50	48	46	44
Quartz sand	10	10	10	10
Re.Wo	-	2	4	6
Total	100	100	100	100

The prepared batches were initially processed through a laboratory-scale simulation of industrial tile manufacture. All raw materials were wet-milled in a porcelain jar mill with dense alumina grinding media for 45 min, using 40 wt.% water (relative to the slip) and 0.3 wt.% sodium tripolyphosphate as deflocculant, referred to the dry batch weight. Particle size distribution was monitored by X-ray monitoring of gravity sedimentation (ASTMC958). The resulting slips were oven-dried, then deagglomerated using a hammer mill equipped with a 500 μm grid. The powders were subsequently manually granulated through a 2 mm sieve to achieve a moisture content of approximately 8 wt.%, in accordance with standard industrial practice. The granulated powders were pressed into tiles of 110 × 55 × 5 mm under a pressure of 40 MPa using a hydraulic press, and subsequently dried in an oven at 105 °C overnight.

The technological behaviour of unfired samples was evaluated through the determination of the following properties: green (once shaped) and dry (after drying) bulk density (weight/volume ratio); green and dry flexural strength (ASTM C648); springback after pressing (i.e., $100(L_p–L_m)/L_m$, where L_p is the length of the pressed tile and L_m is the length of the mold); drying shrinkage (ASTM C326).

The sintering behaviour of the bodies was investigated by *in-situ* experiments on specimens (approximately 5 × 5 × 5 mm) cut from the dry tiles. Isothermal tests were carried out by optical thermo-dilatometry (TA, ODP868, Germany or Expert Lab Service, Misura, Italy) with a heating ramp of 80 °C/min up to 1180 °C and 30 min dwell time. Isothermal sintering kinetics were calculated from early, linear and decreasing shrinkage (derived from specimen height variation) by dwell time at the various maximum temperatures, as described in Figure S1 in supplementary materials of Conte et al. [36]. These *in-situ* tests also allowed the determination of the kinetics in the de-sintering stage, i.e., the stage consisting in an inversion of the sintering process that may occur once the maximum density is reached, leading to a more or less accentuated expansion of the ceramic body. The plateau of stability at T_{max} (i.e., the time between the achievement of maximum densification and the start of bloating) was also determined.

Powder compacts were fast fired in an electric kiln at four different maximum temperature values (T_{max} = 1160, 1180, 1200 and 1220 °C) to follow the technological properties of the tiles. The thermal cycle consisted in a 60 min cold-to-cold cycle and 5 min of dwell time at T_{max}.

Technological properties, determined after firing the specimens at the different T_{max}, were: linear firing shrinkage (i.e., $100(L_m–L_f)/L_m$ where L_f is the length of the fired tiles and L_m is the length of the mold), water absorption, bulk density and open porosity (ASTM C373) and flexural strength (ASTM C648).

On the basis of the results obtained three batches were selected for the scale – up test: the benchmark (BNK_SU), REWO2 (REWO2_SU) and REWO4 (REWO4_SU) formulations. The scale-up test was carried out in the SACMI plant in Imola (BO). The aim of the scale up project was to obtain 500 Kg of spray dried material to produce a set of 33 × 25 tiles to cover 60m^2.

The three batches were realized following the formulation of the lab simulation tests and all the material was milled in smart powder mill MTD500 after the addition of 36% of water and 0.4% of deflocculant (sodium tripolyphosphate). The powders were milled up to residue at 63 μ <0.5 wt.%. The powders were spray dried in a small spray-dry plant (powder humidity 6.5%) and pressed with a PH380 press in 33 × 25 cm format at two different pressures 350Kg/cm^2 and 400 Kg/cm^2. The pressed tiles were dried in ECP 2350/11 drier for 24 h and then were fired in FMP 1600/49 roller kiln at five different temperatures (1180, 1190, 1200, 1210 and 1220 °C) to unravel maximum densification temperature in the new conditions. Once the conditions were optimized in the plant, a set of 60m^2 of tiles was produced in the same conditions.

QPA exploiting Rietveld refinement, following the procedure reported for the raw materials, were performed for samples obtained both at lab scale and in the pilot plant at maximum densification temperature.

The microtextural characterization was performed only on the samples obtained in the pilot plant at maximum densification temperature. The microstructure of the samples was examined using a JSM-6010PLUS/LA SEM microscope equipped with an Energy Dispersive X-ray (EDX) spectrometer (Oxford INCA-350). Operating conditions used were: 20 kV, 10 mm working distance and spot size of 60. For samples preparation, the fired tiles were cut and embedded in an epoxy resin. Subsequently, the surface exposing the tile cross-section was polished and the samples were fixed on Al stubs and coated with a thin film carbon (ca. 10 nm thick) using a Carbon Coater-Balzers CED-010. Both Secondary Electron Images (SEI) and Backscattered Electron Images (BEC) were collected.

2.2. Life cycle assessment study

The Life Cycle Assessment was conducted in accordance with ISO 14,040 [48] and ISO 14,044 [49] regulations. The main assumptions and modelling choices are described below.

2.2.1. Goal and scope definition

The aim of this LCA study is to evaluate and contextualize, from an environmental perspective, the incorporation of inertized mineral wool waste (Re.Wo) as a partial substitute for feldspar in unglazed ceramic tiles produced at industrial scale. The analysis is based on the formulations selected after TRL6 scale-up tests and extends beyond the manufacturing stage to include downstream life cycle stages, such as distribution, use and end-of-life of the finished tile, in order to place environmental contributions from the manufacturing phase in a full life cycle context. The study has two main objectives: (i) to compare the environmental performance of the investigated formulations and assess the extent to which Re.Wo incorporation affects the overall cradle-to-grave burden of an unglazed ceramic tile; (ii) to identify the main environmental hotspots, including those associated with the upstream treatment of mineral wool waste.

2.2.2. System boundaries, function of the system and functional unit

The studied system concerns the industrial-scale production of unglazed ceramic tiles, containing 0–4 wt.% Re.Wo as a partial substitute for sodic feldspar, originally sourced from Turkey. This substitution is intended to reduce the use of virgin raw materials while recycling a locally available secondary raw material derived from mineral wool waste (MWW) treatment. The LCA framework adopted in this work was adapted from Ferrari et al. [50], which presents a cradle-to-grave life cycle model for ceramic tiles including manufacturing, distribution, use and end-of-life stages, developed mainly from primary industrial data. In the present study, this reference framework was modified to represent the specific formulations investigated here and to exclude glazing raw materials and glazing operations, while maintaining the same overall system boundaries. The analysed formulations were BNK_SU (benchmark tile, 0 wt.% Re.Wo), REWO2_SU (2 wt.% Re.Wo) and REWO4_SU (4 wt.% Re.Wo), all based on the pilot-scale batches tested at TRL 6. In addition, a further benchmark formulation, coded BNK_SU_NL, was included to represent a tile with a higher share of extra-EU raw materials. In this case, Clay 1 was assumed to be sourced from Ukraine instead of Italy and Germany. Because Re.Wo is produced through the thermal treatment of hazardous mineral wool waste (MWW) [35,51], the system boundaries also include the upstream MWW management and inertization system. This reflects the attributional approach adopted in the study, whereby Re.Wo carries a share of the environmental burden associated with the waste-treatment process. A graphical representation of the system boundaries for the MWW treatment and inertization system is provided in Fig. 1S.

The functional unit for the cradle-to-grave comparison is defined as 1 m^2 of unglazed ceramic tile, with an average thickness of 7.3 mm, an average mass of 17.4 kg/m^2, and a service lifetime of 50 years [50].

2.2.3. Life cycle inventory (LCI) and life cycle impact assessment (LCIA)

The life cycle inventory of the ceramic tile was derived from Ferrari et al. [50], which includes, for each stage, from raw material extraction to end-of-life, the inputs of materials and energy, transport of raw materials, use of plant and machinery, direct emissions to the atmosphere, and treatment of waste streams. The reference LCI model was mainly built on primary data from a ceramic tile company located in Emilia-Romagna (Italy), with an annual production of 11.8 million m^2 of tiles. In the present study, the manufacturing stage was adapted to the formulations investigated here, based on the batch compositions reported in Table 3S. Compared with the reference model, glazing-related contributions were excluded to reflect the unglazed tiles examined in this work, no recycling of fired tiles was considered, and raw-material transport was updated according to the sourcing scenarios adopted here. Under the BNK_SU_NL configuration, extra-EU raw materials account for 70 wt.% of the formulation. Background processes and secondary inventory data were modelled using the ecoinvent database (v3.10) [52,53].

The model was implemented in SimaPro (v9.6.0.1) [54] using an attributional approach based on the APOS (Allocation at the Point of Substitution) system model [53].

Within this attributional framework, the inertization of mineral wool waste was modelled as a multi-output process, since it simultaneously provides a waste-treatment service and generates the secondary raw material Re.Wo. The environmental burdens of this process were therefore partitioned between these two functions using a mass-based allocation, consistent with the approach previously adopted for asbestos-containing waste inertization [55]. Accordingly, 55.1% of the burdens were assigned to the treatment of MWW from building dismantling and 44.9% to the inertized Re.Wo, which then transfers this share of burden to the ceramic tile.

The inventory of the mineral wool waste management and inertization system includes dismantling and collection of the waste, sealing in plastic big bags, transport to the treatment plant, volumetric reduction, additional sealing with plastic stretch film, temporary storage, and thermal treatment. The inertization process was modelled on the basis of the design of the industrial-scale plant with a treatment capacity of 1 t/h, corresponding to a potential annual treatment of 8760 t of mineral wool waste and the simultaneous production of 7008 t/year of Re.Wo. Specifically, the mineral wool waste, in the form of 1.5 t bales, is

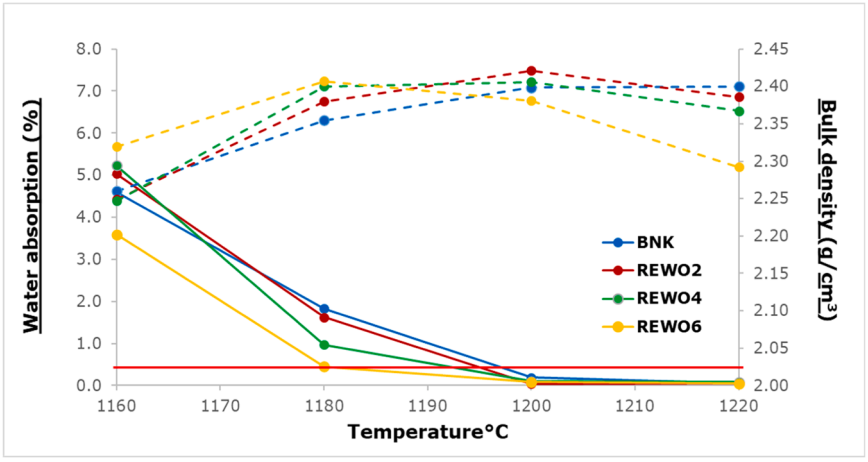

Fig. 1. Gresification curve for all the fired samples realized after the industrial simulation at laboratory scale.

thermally treated in an oxy-combustion furnace operating at about 1000 °C, followed by a flue-gas cleaning section which, in compliance with Best Available Techniques (BAT), includes a post-combustor, an SNCR (Selective Non-Catalytic Reduction) reactor, an adiabatic quenching reactor for gas cooling, a reactor for neutralizing acidic compounds with hydrated lime (Ca(OH)2), a bag filter, and finally an SCR (Selective Catalytic Reduction) reactor.

Primary data for the inertization plant (1 t/h capacity) were provided by the company that patented the process and is expected to operate the industrial unit. These data were complemented by theoretical calculations and selected secondary information, particularly for estimating air emissions from the combustion of the waste and their subsequent abatement in the gas-treatment system.

Potential environmental impacts were quantified using SimaPro (v9.6.0.1) [54] by applying the Environmental Footprint 3.1 (EF 3.1) LCIA method [56], in the version implemented by PRé Consultants (v1.01) [57]. The method provides midpoint indicators for 16 impact categories, consistent with EN 15,804+A2:2019, the European core standard for Environmental Product Declarations (EPDs) in the construction sector [58], except for biogenic CO_2 uptake and emissions. In addition, a normalized and weighted single score, expressed in Points (Pt), was used to summarise the overall environmental burden relative to a reference situation. This score was obtained by applying global normalization factors, thereby converting each impact category into a comparable magnitude in Pt [56]. Subsequently, each normalized score is multiplied by a weighting factor (summing to 1), reflecting the relative environmental importance of each impact category [59].

3. Results and discussion

3.1. Laboratory scale test: TRL4

The technological properties of the semi-finished products reported in Table 5, indicate that all compositions fully comply with the requirements typically accepted for porcelain stoneware, with low shrinkage after pressing and during drying, good bulk density and considerable flexural strength. In particular, flexural strength exhibits values higher than 10.0 kg/cm² in the green state and 28.3 kg/cm² in the dry state, which are regarded as very good in industrial practice. All values measured for the Re.Wo-bearing compositions are closely comparable with those of the benchmark batch, as the deviations fall within the experimental error for all the parameters considered.

When the benchmark composition based on local raw materials is compared with the standard batch prepared using conventional Ukrainian ball clays [35], the former exhibits slightly lower density in both the green state (2.052 *vs.* 2.173 g/cm³) and the dry state (1.927 *vs.* 2.016 g/cm³). This behaviour is consistent with the different particle-size distributions of the two batches, with a d_{50} of about 4 μm for the new benchmark and about 5.5 μm for the Ukrainian-based composition. As reported in the literature, a decrease in particle size may lead to lower bulk density [60], since a less sorted particle size distribution allows for a more efficient powder compaction [61]. Nevertheless, these differences do not hinder the achievement of comparable flexural strength, either in the green state (10.2 *vs.* 9.4 kg/cm²) or in the dry state (28.4 *vs.* 28.5 kg/cm²). Indeed, since all tiles were formed at the same pressure (40 MPa), and since bulk density decreases with decreasing particle size, as observed for the new benchmark, the retention of essentially unchanged mechanical strength actually indicates a higher intrinsic strength of the new benchmark [62]. These results indicate that the replacement of imported clays with local raw materials does not compromise the technological quality of the semi-finished products. Furthermore, the addition of Re.Wo does not significantly affect the properties of the unfired bodies. All the values listed in Table 5, in fact, fall within the range commonly accepted in industrial practice.

The tiles produced at laboratory scale were fired at different temperatures to determine the temperature T (°C) corresponding to maximum densification, which was then adopted as the reference starting point for the scale-up process. The corresponding values of water absorption, bulk density and open porosity are reported in Table 6 and shown in Fig. 1. Other technological properties of the fired bodies,

Table 5
Technological properties of unfired products at the laboratory scale.

		unit	BNK			REWO 2			REWO 4			REWO 6		
Slip	Particle size (d_{50})	μm	3.95		-	4.18		-	4.50		-	4.46		-
Green	**springback after pressing**	%	0.42	±	0.01	0.41	±	0.01	0.40	±	0.02	0.40	±	0.01
	bulk density	g/cm³	2.052	±	0.031	2.031	±	0.024	2.044	±	0.010	2.058	±	0.020
	flexural strength	Kg/cm²	10.2	±	0.6	10.3	±	0.1	10.0	±	0.5	10.4	±	0.4
Dry	**drying shrinkage**	%	0.03	±	0.01	0.02	±	0.01	0.01	±	0.01	0.04	±	0.01
	bulk density	g/cm³	1.927	±	0.030	1.915	±	0.019	1.922	±	0.009	1.930	±	0.025
	flexural strength	Kg/cm²	28.4	±	0.7	28.5	±	1.0	28.4	±	0.5	28.3	±	1.1

Table 6
Technological properties of finished products fired at different temperatures at the laboratory scale (W.A.= Water absorption; B.D.= Bulk density; O.P. = Open porosity).

Batch	property	unit	T max (°C)							
			1160		1180		1200		1220	
BNK	**W.A.**	%	4.60	± 0.30	1.83	± 0.20	0.19	± 0.09	0.05	± 0.02
	B.D.	g/cm^3	2.260	± 0.015	2.354	± 0.013	2.398	± 0.012	2.400	± 0.002
	O.P.	%	10.40	± 0.60	4.30	± 0.55	0.45	± 0.18	0.13	± 0.06
REWO2	**W.A.**	%	5.03	± 0.10	1.62	± 0.04	0.04	± 0.01	0.06	± 0.02
	B.D.	g/cm^3	2.249	± 0.002	2.380	± 0.014	2.421	± 0.002	2.386	± 0.004
	O.P.	%	11.32	± 0.04	3.86	± 0.09	0.18	± 0.01	0.15	± 0.05
REWO4	**W.A.**	%	5.23	± 0.40	0.96	± 0.08	0.10	± 0.04	0.08	± 0.04
	B.D.	g/cm^3	2.247	± 0.007	2.400	± 0.006	2.406	± 0.001	2.367	± 0.004
	O.P.	%	11.74	± 0.70	3.21	± 0.31	0.24	± 0.08	0.18	± 0.10
REWO6	**W.A.**	%	3.59	± 0.20	0.45	± 0.14	0.08	± 0.03	0.05	± 0.02
	B.D.	g/cm^3	2.319	± 0.001	2.407	± 0.003	2.381	± 0.014	2.292	± 0.015
	O.P.	%	8.32	± 0.45	1.08	± 0.35	0.20	± 0.08	0.11	± 0.04

such as flexural strength and linear shrinkage, are presented in the scale-up section, where they are more relevant to the higher-TRL assessment of the process.

The addition of Re.Wo clearly changes the properties of the fired bodies. Up to 1180 °C, all Re.Wo-bearing samples show higher bulk density than the benchmark. At 1200 °C, this trend is still observed for REWO2 and REWO4, whereas REWO6 begins to exhibit a decrease in bulk density. At 1220 °C, all Re.Wo-containing tiles display a bulk-density reduction, the extent of which is proportional to the amount of waste added. This behaviour is clearly attributable to bloating associated with tile overfiring, an effect that is more pronounced in REWO6 [36]. By contrast, the benchmark composition shows a continuous increase in bulk density up to the highest temperature investigated, indicating excellent thermal stability. Water absorption decreases in all cases as densification proceeds, and all samples reach values below 0.5 wt.% at 1200 °C. Based on these technological results, the temperature of maximum densification (T_{md}) can be identified as 1200 °C for BNK, REWO2 and REWO4, and 1180 °C for REWO6. However, in the latter case it should be noted that, although the water absorption at 1180 °C is low enough to meet the ISO 13,006:2018 requirement for porcelain stoneware classification, it is not optimal for the industrial production of high-quality materials. Conversely, at higher temperatures, although water absorption decreases further, clear signs of overfiring are observed. Accordingly, REWO6 was not considered suitable for further scale-up, since the laboratory results identified this composition as lying beyond the most favourable processing window under the selected formulation and firing conditions.

A comparison between the benchmark composition investigated in this study and that reported by Arletti et al. (2023) [35] shows that the use of local raw materials leads to improved properties of the fired product. In particular, the optimum firing temperature decreases from 1240 °C to 1200 °C, while the bulk density at the temperature of maximum densification (corresponding to W.A. <0.5%) increases from 2.336 to 2.398 g/cm^3. These improvements—namely the lower firing temperature and the enhanced densification efficiency—can be attributed both to differences in chemical composition and to particle-size distribution. Specifically, the local formulation is richer in alkali and alkaline-earth oxides and slightly poorer in silica and alumina than the batch based on Ukrainian raw materials (see Table 2S). In addition, it exhibits a finer particle-size distribution, with a d_{50} of ~4 μm compared with about 5.5 μm for the Ukrainian batch. The finer particle size promotes sintering by accelerating reaction kinetics, ultimately resulting in a better-densified ceramic body [62]. This comparison is intentional and is not meant to prove direct equivalence between the two formulations, but addresses one of the aims of the present work: verify whether technologically satisfactory porcelain stoneware bodies can still be obtained when the previous Ukrainian-clay-based formulation is replaced by a more regionally sourced raw-material set.

Hot-stage microscope (HSM) analyses were carried out under isothermal conditions at 1180 °C to investigate the sintering behaviour of the bodies. A detailed mechanistic investigation of the effect of Re.Wo on the extent of the sintering stages, sintering kinetics, efficiency of densification, melt-related behavior and microstructural development was previously reported for a different porcelain stoneware system based on Ukrainian clays [36]. In the present work, HSM was used to compare the thermal behaviour of the new formulations and to derive quantitative kinetic parameters from the shrinkage curves. These parameters are reported in Table 7. The start of densification falls within a relatively narrow temperature interval, between 1000 and 1026 °C, indicating that all compositions exhibit a broadly comparable thermal response during heating. A clearer distinction emerges from the sintering-rate analysis at 1180 °C. BNK, REWO2 and REWO4 show overall comparable kinetics, with total sintering rates of 0.31, 0.34 and 0.31 min^{-1}, respectively. Their early-stage rates range from 0.81 to 0.94 min^{-1}, the constant-stage rates from 1.61 to 1.66 min^{-1}, and the decreasing-stage rates from 0.15 to 0.17 min^{-1}. These data indicate that low Re.Wo additions do not substantially modify the overall densification behaviour at 1180 °C. In contrast, REWO6 exhibits a clearly different behaviour. This composition shows the highest early-stage, constant-stage and decreasing-stage rates, equal to 1.00, 1.97 and 0.23 min^{-1}, respectively, resulting in a markedly higher total sintering rate of 0.51 min^{-1}. However, this faster densification does not correspond to a wider or more stable firing window. On the contrary, REWO6 is the only composition displaying a finite stability plateau at 1180 °C, lasting 450 s (7.5 min), followed by measurable bloating, as indicated by the inversion of the HSM curve and by a bloating rate of 0.05 min^{-1}. Therefore, REWO6 is more appropriately interpreted as a composition showing accelerated sintering accompanied by reduced thermal stability and an earlier transition towards overfiring, rather than as a body simply characterised by a beneficially stronger fluxing action. In the previously

Table 7
Sintering parameters of porcelain stoneware bodies at 1180 °C (*e.u.* = experimental uncertainty).

	Unit	BNK	REWO2	REWO4	REWO6	*e.u.*
Start of densification	°C	1006	1026	1000	1025	*5*
Early-stage rate	min^{-1}	0.87	0.94	0.81	1.00	*0.02*
Constant-stage rate	min^{-1}	1.61	1.64	1.66	1.97	*0.03*
Decreasing-stage rate	min^{-1}	0.15	0.17	0.16	0.23	*0.02*
Sintering rate (total)	min^{-1}	0.31	0.34	0.31	0.51	*0.02*
Stability plateau	s	-	-	-	450	*1.00*
Bloating rate	min^{-1}	-	-	-	0.050	*0.001*

investigated Re.Wo-bearing system, this behaviour was interpreted in terms of progressive interaction between the waste-derived glass and the ceramic melt, with crystallization of Fe- and Ca-Mg-Fe-rich phases from the Re.Wo at intermediate temperature followed by their dissolution at higher temperature, which modified the melt properties and accelerated densification kinetics [36].

The mineralogical composition of the tiles produced at laboratory scale was evaluated at the temperature of maximum densification (Table 8). The most marked variation concerns the feldspar content. In REWO6, plagioclase accounts for 16.6 wt.%, whereas in the compositions with lower Re.Wo additions it is present only in the 4–5 wt.% range. At the same time, mullite content decreases progressively with increasing Re.Wo incorporation. This trend is consistent with previous findings [36], which showed that higher Re.Wo contents favour higher residual feldspar and lower mullite formation. This behaviour can be attributed to the peralkaline character of Re.Wo, which is richer in alkali and alkaline-earth cations (named Na and Ca) than in Al (on a molar basis). As a consequence, the overall batch composition shifts from the peraluminous towards the peralkaline field, increasing feldspar stability and hindering mullite formation [36]. More generally, the efficiency of mullite formation from the Al_2O_3 released by kaolinite and illite, as well as its preservation after firing, depends not only on the clay minerals themselves but also on the total alumina content of the batch and its ratio to alkalis [15,63]. In addition, the relatively high Ca content of Re.Wo could favour the formation of phases competing with mullite, such as anorthite or augite. No clear evidence of these phases was detected by XRPD, nevertheless, the presence of anorthite cannot be completely ruled out, since its detection and quantification are extremely challenging when present in combination with albite [36,64]. Anyway, a detailed distinction among the two phases was out of the scope of this work. It should also be noted that the addition of 6 wt.% Re.Wo lowers the temperature of maximum densification. As a result, at 1180 °C feldspar decomposition is interrupted at an earlier stage, and the higher residual feldspar content observed in REWO6 corresponds to a lower amount of glassy phase in the fired body. This phase assemblage indicates that the higher Re.Wo. addition does not simply enhance a fluxing behaviour, but rather shifts the vitrification path towards a less favourable and less thermally stable regime under the selected firing conditions.

On the basis of the laboratory-scale results, BNK, REWO2 and REWO4 were selected for the subsequent TRL 6 scale-up phase. REWO6 was not advanced further because it was identified as lying beyond the most suitable processing window under the selected formulation and firing conditions, owing to its reduced thermal stability, altered phase evolution and earlier onset of overfiring.

Table 8
Quantitative phase analyses of the tiles produced in Laboratory and fired at the T_{md} (with ± errors) obtained after Rietveld refinement and refinement agreement indices.

	BNK-1200 °C	REWO2–1200 °C	REWO4–1200 °C	REWO6–1180 °C
Rietveld agreement indices				
R_p (%)	4.70	4.38	4.41	4.85
R_{wp} (%)	7.00	6.13	6.19	6.71
χ^2	2.964	2.243	2.287	2.725
Phase (wt.%)				
Quartz	21.0(2)	19.0(2)	20.9(2)	18.2(2)
Mullite	9.4(3)	8.2(2)	7.5(2)	7.5(3)
Plagioclase	5.2(1)	5.2(1)	4.3(2)	16.6(2)
Rutile	0.19(5)	0.22(4)	0.18(4)	0.05(5)
Amorphous phase	64.2(4)	67.4(3)	67.2(4)	57.7(4)

3.2. Scale up test: TRL 6

All tests were performed at the SACMI pilot plant in Imola (BO), following the procedure described in Section 2. Slip properties were monitored throughout the milling stage, and the corresponding values recorded at each check point are reported in Table 4S of the Supplementary Materials. After about 10 h of milling, the residue on the 63 μm sieve decreased to ≤0.5 wt.% for all batches, and milling was therefore stopped. Water content remained essentially constant during milling, at approximately 35 wt.% for all compositions, whereas slip density was slightly higher in the Re.Wo-bearing batches. Final slip viscosity increased slightly with Re.Wo content, from 2.0 °E in the benchmark to 2.2 and 2.3 °E in REWO2_SU and REWO4_SU, respectively, possibly owing to ion leaching from the glass during wet processing, as previously reported for waste-glass-containing ceramic slips [65]. The slips were then spray-dried, yielding powders with a final moisture content of 6.5 wt.% in all cases. Overall, 250 kg of spray-dried powder was produced for BNK_SU, whereas 500 kg was produced for each of REWO2_SU and REWO4_SU. The powders were subsequently pressed at 350 and 400 kg/cm^2 in order to evaluate the effect of forming pressure on powder compaction and, in turn, on degassing, densification and possible black-core formation during firing [66].

The technological properties of the green and dry semi-finished products are reported in Table 5S of the Supplementary Materials. For all compositions, increasing the forming pressure resulted in higher green and dry density and, correspondingly, higher flexural strength. At the same pressure, the Re.Wo-bearing bodies also showed slightly higher density and strength than the benchmark, in agreement with their coarser particle-size distribution (Table 4S, supplementary materials). Overall, the addition of Re.Wo did not negatively affect the technological behaviour of the unfired bodies. Compared with the laboratory-scale specimens, the mechanical strength of the pilot-plant tiles was only slightly lower in the green state, within experimental uncertainty, whereas it was clearly higher after drying. This difference can reasonably be attributed to the different powder preparation route: unlike laboratory granulation, spray drying produces granules with more regular morphology, narrower size distribution and better flowability, thereby improving packing during pressing, increasing density homogeneity and ultimately enhancing the mechanical performance of the dried bodies.

In the present pilot-scale assessment, the densification behaviour of the ceramic bodies is primarily evaluated through their technological parameters (bulk density, water absorption, shrinkage and flexural strength), complemented by pyroplastic deformation as an indirect indicator of high-temperature stability and SEM/EDS observations on the selected pilot-scale products. Therefore, after pressing and drying, the tiles were fired at maximum temperatures between 1180 and 1220 °C to follow the evolution of their technological properties over the investigated firing range. Bulk density and linear shrinkage are summarised in Fig. 3, while the gresification curves are shown in Fig. 4 and reported in Table 6S of the Supplementary Materials, together with the values of pyroplastic deformation and flexural strength at each temperature.

As shown in Figs. 3a and 4, increasing the forming pressure generally led to slightly higher fired bulk density and lower water absorption, particularly at temperatures below the temperature of maximum densification, where the effect of the initial packing state is still significant. However, consistently with previous observations on porcelain stoneware [62], the influence of forming pressure on the fired properties was much less pronounced than in the unfired state, indicating that the lower initial compaction was largely recovered during firing. In other words, although tiles pressed at lower pressure started from a lower dry bulk density, liquid-phase sintering progressively compensated for this difference as firing proceeded. This interpretation is also supported by the shrinkage behaviour (Fig. 3b). Linear shrinkage systematically decreased with increasing forming pressure and was therefore inversely related to dry bulk density [62]. Nevertheless, higher shrinkage did not

necessarily correspond to better densification. For example, the benchmark composition pressed at 350 kg/cm^2 showed markedly higher shrinkage than the same body pressed at 400 kg/cm^2, whereas the corresponding difference in fired bulk density remained relatively limited, because the initial packing gap was progressively compensated during firing. This indicates that part of the additional shrinkage simply reflects the need to compensate for the lower initial packing of the dry body. This is true for all the batches here considered. At the same time, the present results are consistent with the microstructural effect described for differently compacted porcelain stoneware bodies: when the amount and composition of the melt do not vary substantially, a higher initial porosity may provide more space for liquid-phase redistribution and pore filling, thereby allowing slightly faster densification kinetics and a partial recovery of the initial compaction gap during firing [62]. Therefore, shrinkage alone cannot be regarded as a direct indicator of densification efficiency, since it reflects both the initial packing state and the subsequent sintering response.

The firing behaviour of the pilot-scale tiles is more clearly illustrated by Fig. 4, where water absorption and bulk density are plotted as a function of temperature for the three compositions and the two forming pressures. A first general observation is that all compositions follow the typical gresification trend: with increasing firing temperature, water absorption decreases sharply, while bulk density increases up to a maximum and then tends either to stabilise or to decrease slightly when overfiring begins. However, the onset and extent of these changes depend mainly on composition, while forming pressure exerts a secondary effect, most evident at the lower end of the investigated firing range.

For the benchmark composition, water absorption is still relatively high at 1180 °C, with pressure-dependent differences still visible, then drops markedly between 1180 and 1190 °C, and becomes nearly null at 1200 °C and above, where differences between the two forming pressures become negligible. At the same time, bulk density increases progressively from 1180 to 1200–1210 °C, where it reaches its highest values, and then remains nearly stable up to 1220 °C, with only a very limited decrease. This behaviour indicates a relatively stable firing interval within the investigated temperature range, since the body continues to densify efficiently up to 1200–1210 °C and does not show clear evidence of pronounced overfiring even at the highest investigated temperature.

REWO2_SU shows a very similar overall trend, confirming that the addition of 2 wt.% Re.Wo does not substantially alter the firing behaviour of the benchmark. Water absorption decreases rapidly with temperature and approaches zero at 1200 °C, while bulk density increases steadily up to 1200–1210 °C for both tiles pressed at 350 and 400 kg/cm^2. Compared with the benchmark, REWO2_SU appears to undergo slightly earlier densification, especially at the higher forming pressure, while its thermal stability is only marginally reduced at the highest investigated temperature, as indicated by the slight decrease in bulk density at 1220 °C. Overall, these results confirm that the 2 wt.% addition preserves a firing behaviour fully compatible with the investigated pilot-scale processing conditions.

A more evident effect is observed for REWO4_SU. In this composition, water absorption is already significantly lower at 1180 °C than in the other bodies, indicating that densification starts earlier, consistently with the fluxing role previously observed for Re.Wo-containing bodies [35,36]. Between 1180 and 1190 °C, water absorption drops rapidly to values close to zero, showing that the gresification threshold is reached at lower temperature. At the same time, bulk density increases rapidly and reaches its maximum at around 1200 °C. Beyond this temperature, however, the trend changes: a clear decrease in bulk density is observed at 1210 °C and becomes even more evident at 1220 °C. Therefore, although REWO4_SU densifies earlier, it also enters the overfiring regime earlier than the other compositions. In other words, the addition of 4 wt.% Re.Wo shifts the densification process towards lower temperature, but also narrows the useful firing window, regardless of the applied forming pressure.

Overall, Fig. 4 confirms that BNK_SU and REWO2_SU reach maximum densification in the 1200–1210 °C range and retain good thermal stability, whereas REWO4_SU undergoes earlier densification but also an earlier loss of stability. On this basis, 1200 °C can be regarded as the most suitable compromise firing temperature for the pilot-scale production, since it ensures negligible water absorption for all compositions while still avoiding the more evident onset of overfiring observed at higher temperature, especially for REWO4_SU.

The pyroplastic index (Table 6S, supplementary materials) increases with temperature, as expected, but does not show a simple monotonic dependence on forming pressure, and its response is clearly composition-dependent. In the present case, the parameter does not provide an unambiguous criterion for discriminating among the investigated processing conditions, although it generally confirms the lower high-temperature stability of the more fluxed compositions. Nevertheless, the variations among the different batches are extremely slight. Moreover, although this parameter does not provide a direct rheological quantification of the body viscosity at high temperature, it offers a useful indirect indication of deformation tendency under firing conditions representative of the pilot-scale tests.

Flexural strength values reported in Table 6S range from about 478 to 603 kg/cm^2, corresponding to approximately 47–59 MPa, and are therefore always well above the minimum reference value of 35 MPa for porcelain stoneware. This confirms that all investigated compositions meet the required mechanical standard over the whole firing range. Differences among compositions are relatively limited: BNK_SU generally shows the highest values, whereas REWO2_SU and REWO4_SU remain broadly comparable and do not exhibit any systematic loss of strength due to Re.Wo addition. Thus, despite the earlier onset of overfiring observed for REWO4_SU based on bulk density and water absorption, the mechanical performance of the fired tiles remains fully satisfactory within the investigated temperature range.

On the basis of the overall technological results, and especially in view of the possible subsequent production of glazed tiles, the specimens pressed at 350 kg/cm^2 were selected for further characterization, including mineralogical analysis and SEM investigation. This condition was preferred as a more conservative processing option, since a lower degree of compaction may favour degassing of the body during firing and thereby limit glaze defects related to gas entrapment after glaze sealing, such as bubbles and pinholes [67]. Therefore, to complement the technological data and provide direct microstructural support to the interpretation of the pilot-scale firing behaviour, QPA and SEM/EDS analyses were carried out on the selected specimens pressed at 350 kg/cm^2 and fired at 1200 °C.

The QPA results are reported in Table 7S and summarised in Fig. 5 together with the corresponding laboratory-scale data. At pilot scale, REWO2_SU and REWO4_SU show very similar phase assemblages and both differ slightly from BNK_SU. In particular, the Re.Wo-bearing bodies are characterised by somewhat lower quartz and mullite contents and by slightly higher residual plagioclase than the benchmark, while the amorphous phase is correspondingly higher. This trend is consistent with the behaviour previously observed in porcelain stoneware containing Re.Wo [36], where the increasing interaction between the waste-derived glass and the ceramic matrix was shown to affect quartz and mullite stability and, at the same time, to favour the persistence of a higher feldspathic fraction. It is worth noting that the reference to previous Re.Wo-bearing systems is not intended to imply strict quantitative equivalence, but rather to highlight qualitative coherence in the observed trends. Although differences in raw-material set and particle-size distribution prevent direct comparison of absolute values, the parallel remains useful for assessing whether the direction of the effects induced by Re.Wo is maintained across different formulation and processing contexts.

The comparison between laboratory- and pilot-scale products of this study shows that the relative differences among compositions are

broadly preserved after scale-up, but the whole system is shifted towards a higher degree of vitrification. In fact, all pilot-scale samples exhibit lower amounts of residual crystalline phases, especially plagioclase, and higher amorphous contents than the corresponding laboratory-scale specimens. Therefore, the scale-up does not alter the general effect of Re.Wo on phase evolution, but rather enhances the overall extent of reaction and vitrification.

These differences cannot be straightforwardly ascribed to grain size distribution or compaction alone. In fact, the laboratory-scale powders were finer than the pilot-scale ones (Tables 5 and 4S, supplementary materials) and were also pressed at a higher pressure (40 MPa versus 35 MPa). According to previous studies [62] a finer particle-size distribution tends to favour vitrification, whereas powder compaction has only a limited influence on the final phase assemblage. Therefore, if granulometry and pressing pressure were the dominant factors, the laboratory-scale samples would be expected to show, if anything, a higher degree of vitrification. Since the opposite is observed, the higher amorphous fraction and lower content of residual plagioclase measured at pilot scale are more plausibly related to the different powder-preparation route and to the non-equivalent thermal histories of the two firing systems. In this respect, the difference between manual granulation and spray drying is likely to be particularly important. In the laboratory route, the slip was first oven-dried and then deagglomerated and granulated mechanically. During this sequence, part of the homogeneity of the suspension may be lost, because drying can promote grain size and phase segregation within the dried batch, while subsequent hammer milling may leave locally coarser aggregates or incompletely remixed domains. By contrast, spray drying tends to preserve the composition of the slip more faithfully within each granule, yielding a more intimate and homogeneous distribution of the batch components. This may favour a more uniform reaction progress during firing and, consequently, a more extensive vitrification. At the same time, the laboratory and pilot products were fired in very different systems, namely a static chamber furnace and a 60 m long industrial roller kiln, respectively. Even when the same nominal maximum temperature is adopted, these two systems cannot be assumed to provide the same effective thermal treatment, owing to differences in heat-transfer efficiency, temperature gradients and overall thermal exposure. Under these conditions, the larger vitrification observed at pilot scale is better interpreted as the result of a more effective overall processing route than as the direct consequence of the nominal firing temperature itself.

Overall, Fig. 5 confirms two main points. First, the Re.Wo-bearing bodies maintain at pilot scale a phase evolution consistent with that already observed at laboratory scale and in the previous Re.Wo study, namely a tendency towards lower quartz and mullite and a slightly greater persistence of feldspar phases compared with the benchmark. Second, scale-up leads to a generally higher degree of vitrification in all compositions, as shown by the increase in amorphous phase and the concomitant decrease in residual plagioclase.

The microstructure of the pilot-scale tiles fired at 1200 °C was investigated by backscattered Scanning Electron Microscope images (Fig. 6a,c,b). All the analysed samples exhibit the typical microstructure of porcelain stoneware at maximum densification, consisting of a continuous vitreous matrix containing relict crystalline phases and a residual closed porosity mainly made up of rounded, isolated pores. The crystalline relics can be mainly ascribed to quartz and feldspar phases, in agreement with the quantitative phase analysis, whereas mullite, as the only newly formed phase, is usually too finely dispersed to be clearly observed unless the polished surface is acid-etched [68]. The pore morphology, in turn, indicates that the bodies are already highly densified and are no longer characterised by significant open and interconnected porosity. Among the three compositions, BNK_SU (Fig. 6a) shows the most homogeneous microstructure, with a relatively uniform glassy matrix and a regular distribution of residual crystals and pores. The Re.Wo-bearing bodies, REWO2_SU and REWO4_SU (Fig. 6b, c), remain overall well densified, but differ from the benchmark by the presence of scattered high-backscattering regions, indicating local enrichment in elements with higher average atomic number. These bright domains are more evident in REWO4_SU and are reasonably attributed to Re.Wo-derived regions, i.e. domains where the contribution of the waste-derived component is still locally recognisable after firing. In this respect, the pilot-scale observations are fully consistent with the behaviour previously described for Re.Wo-containing porcelain stoneware [36], where the waste-derived glass was shown to interact progressively with the ceramic matrix during firing, while still leaving locally distinguishable Fe–Ca–Mg-enriched domains at 1200 °C.

This interpretation is supported by the higher-magnification image and the EDS spectrum reported in Fig. 7 for REWO4_SU. The analysed bright region shows the characteristic elements of Re.Wo., namely Ca, Fe and Mg, together with the major constituents of the surrounding ceramic matrix. Therefore, rather than corresponding to completely unmelted particles sharply separated from the body, these areas are more appropriately interpreted as Re.Wo.-derived relic domains and/or local diffusion halos enriched in waste-related components. This is again in agreement with the previous microstructural study, which showed that, at 1200 °C, the interaction between Re.Wo. and the ceramic matrix becomes significant, although still locally heterogeneous.

At the same time, the absence of extensive pore coarsening or large clusters of bloating pores indicates that, at the investigated additions of 2 and 4 wt.%, the heterogeneity introduced by Re.Wo. does not compromise the overall compactness of the fired body. In other words, the waste-derived component remains microscopically detectable, especially in REWO4_SU, but its presence is still compatible with the development of a dense stoneware microstructure. This observation is in line with the previous Re.Wo. study, which showed that the most critical microstructural effects, such as marked pore coarsening and bloating, become relevant only at higher Re.Wo. contents and/or under clear overfiring conditions.

3.3. LCA results

A prospective LCA was carried out to contextualize, from an environmental perspective, the possible industrial implementation of the formulations selected at TRL 6. In line with the technological focus of the present manuscript, this analysis is intended as a supporting element rather than as a primary result of the study, and is mainly used to identify the main environmental hotspots associated with the proposed valorisation route. Potential environmental impacts calculated at midpoint-level (EF 3.1) for the full life cycle of 1 m^2 of each tile formulation (BNK_SU_NL, BNK_SU, REWO2_SU, and REWO4_SU) are reported in Table 8S of the Supplementary Material. In Fig. 8, results are shown after normalization and weighting of the midpoint-level environmental impact results, expressed as an environmental score in Pt.

Compared to BNK_SU_NL, which contains 70 wt.% extra-EU raw materials, the proposed benchmark tile BNK_SU, composed predominantly of local and EU raw materials (with the exception of Turkish feldspar), showed a reduction in environmental impacts ranging from 0.2% to 9.6%, depending on the impact category considered (Table 8S, supplementary materials). This corresponds to an overall 4% reduction in the normalized and weighted environmental score. These results highlight the importance of prioritizing local raw materials, which served as the baseline for this study to further explore the incorporation of the locally sourced secondary raw material Re.Wo as a substitute for Turkish feldspar.

As shown in Fig. 2S Supplementary Material, and consistently with the results previously reported in [50], the life cycle stages contributing most to the environmental score of 1 m^2 of the benchmark unglazed tile (BNK_SU) are distribution (24.5%), body raw materials (22.4%), use phase (14.7%), and installation (14.2%), while the firing stage accounts for just 5.9%. The dominant role of the distribution stage is primarily driven by the long-distance transport required to deliver finished tiles across Italy, Europe, and other destinations outside Europe, via road

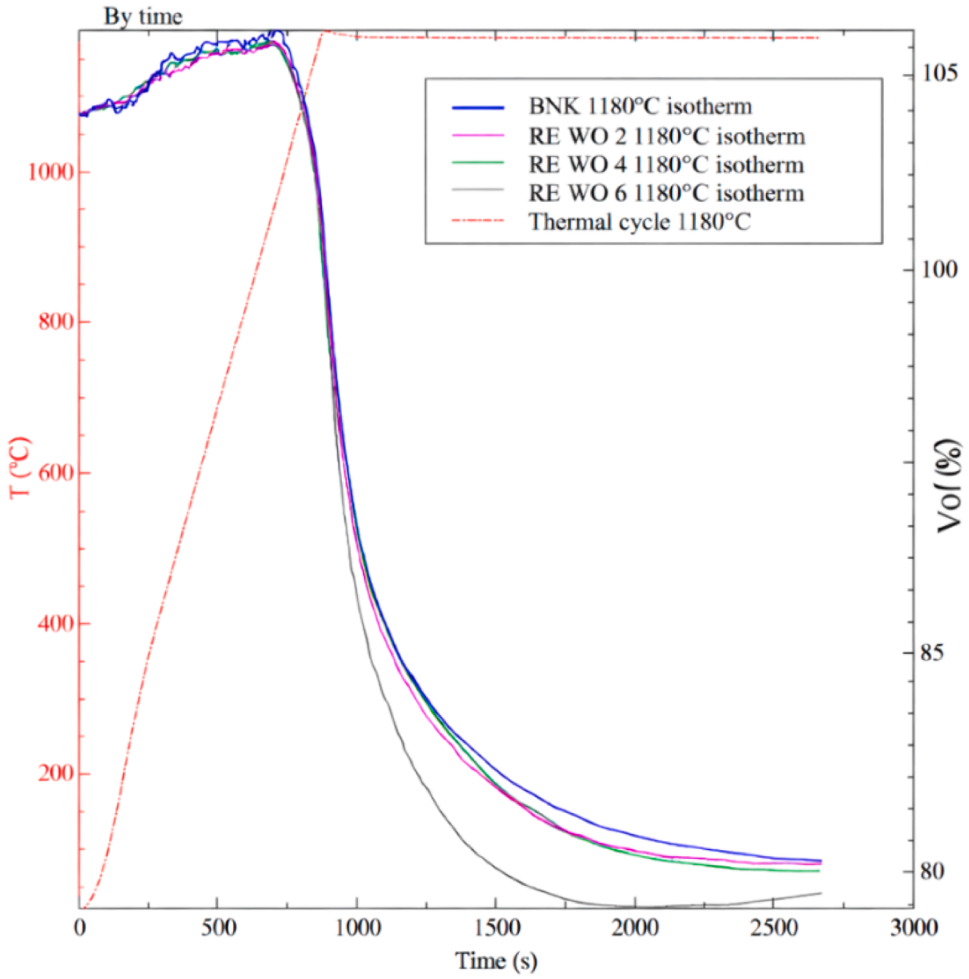

Fig. 2. Thermal behaviour of the ceramic batches (30 min dwell time at 1180 °C). Colour codes: blue: BNK; pink: REWO2; green: REWO4; grey: REWO6; red: thermal cycle.

freight, rail, and sea freight. Transport is also identified as the key driver within the body raw material supply chain, particularly the long-distance sea transport of Turkish feldspar to the ceramic plant, which alone accounts for 37.9% of the raw material supply burden. Additional contributions arise from the transports of the other raw materials, while the one associated with the extraction of raw materials itself remains limited. Among all raw material supply chains, Turkish feldspar extraction and processing carries the highest share at 8.8%. For the use phase, the main upstream contributions stem from water and detergent consumption required to maintain the tile over its 50-year lifetime, while the installation phase is almost entirely dominated (90.8%) by the use of light mortar and its associated upstream production.

Overall, the incorporation of Re.Wo results in limited changes in environmental performance across most impact categories. This is particularly evident for REWO4_SU, the formulation with the highest Re. Wo content, for which the differences relative to BNK_SU remain below 7% in 14 out of 16 impact categories (Table 8S, supplementary materials). More marked deviations are confined to only two categories, namely freshwater eutrophication and ionising radiation, suggesting that the overall environmental effect of Re.Wo incorporation remains modest within the investigated compositional range. Moreover, in light of the uncertainties associated with the overall LCA model, including those arising from the LCIA phase, for which differences of 5–10% are usually the minimum required for relatively robust categories such as climate change, while differences of at least one order of magnitude are required for toxicity and ecotoxicity categories [69], the observed increases for REWO4_SU can still be regarded as limited. Therefore, larger differences would be required to support a more robust claim that the incorporation of Re.Wo determines a significant change in the environmental burden of the ceramic tile across its entire life cycle.

Although Re.Wo has been used as a partial substitute for Turkish feldspar, whose supply and transport emerged as one of the highest contributors to the overall life cycle environmental burden, its incorporation as a secondary raw material led to a slight net increase in the environmental burden. This indicates that, under the present modelling assumptions, the reduced consumption and long-distance transport of Turkish feldspar are offset by the environmental burden associated with Re.Wo. This increase is mainly attributable to the fact that Re.Wo carries almost half of the total burden associated with the mineral wool waste treatment system via inertization, in accordance with the attributional approach used to handle the multifunctionality of the waste treatment process. Among all phases required to collect, prepare, and treat mineral wool waste, the thermal treatment step alone determines nearly all of this contribution (97%), due to its highly energy-intensive nature.

Within the inertization step specifically, as illustrated by the relative contributions to the normalized and weighted environmental score for the inertization of 1 kg of MWW reported in Fig. 3S (supplementary materials), the largest share is associated with the direct consumption of liquid oxygen for the oxy-combustion process (47.2%), followed by natural gas consumption (24.1%), direct emissions to air (23.5%), and the operation of the exhaust gas treatment section (4.8%). This result indicates that the production of liquid oxygen is an important contributor within the inertization system, mainly because of the electricity

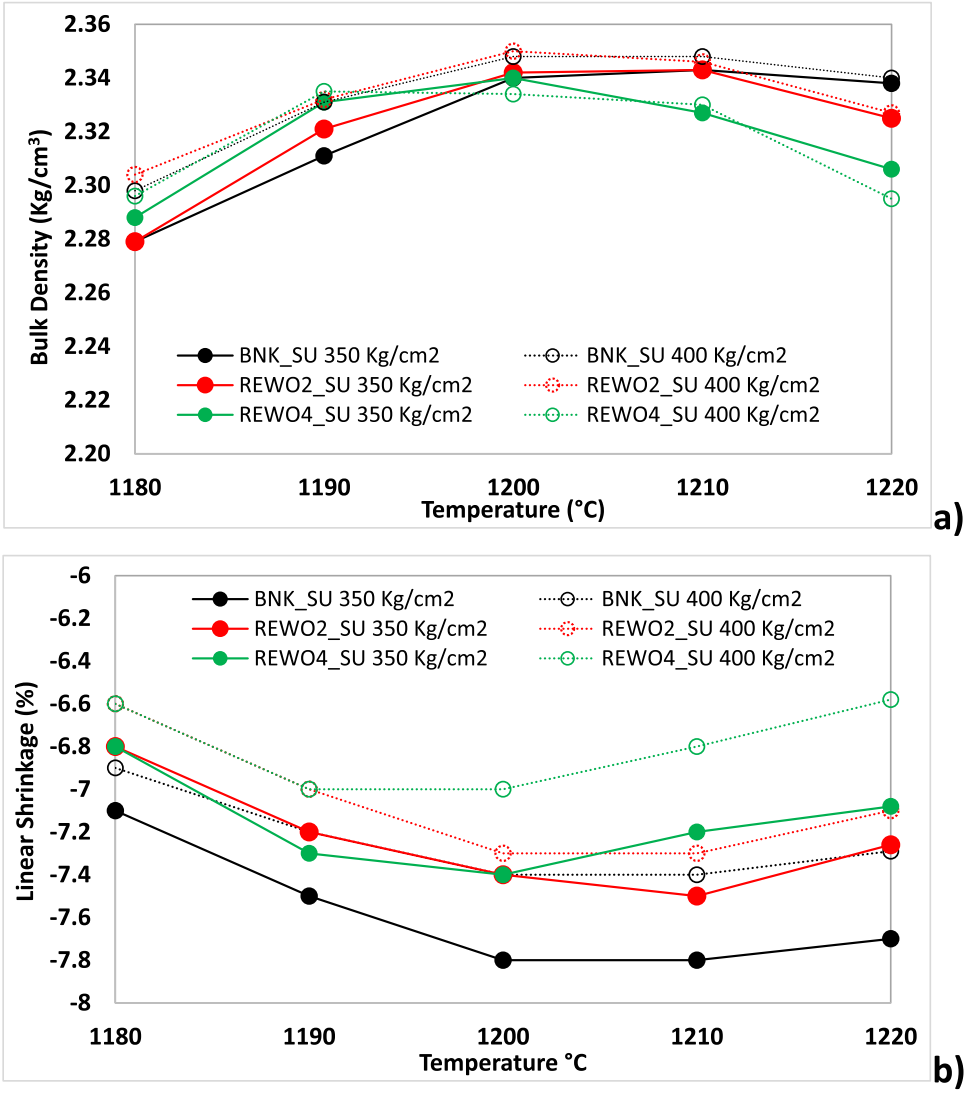

Fig. 3. Variation of Bulk density (a) and linear shrinkage (b) for the tiles at all the investigated T.

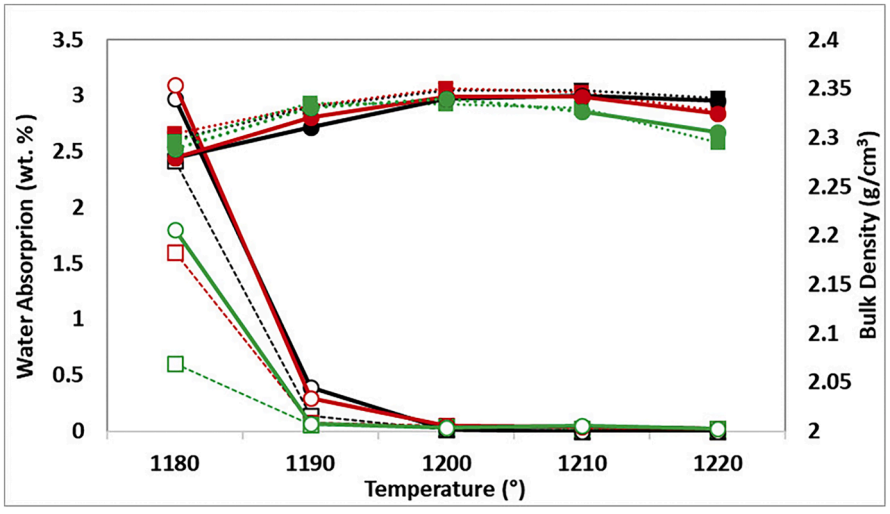

Fig. 4. Gresification curves from the tiles pressed at 350 kg/cm^2 (circles-full lines) and 400 kg cm^2 (squares-dashed lines). Full and empty symbols represent bulk density and water absorption, respectively. Color codes: black BNK_SU, red: REWO2_SU, green: REWO4_SU.

required for its generation, and that its influence is reflected especially in impact categories such as climate change, freshwater eutrophication,

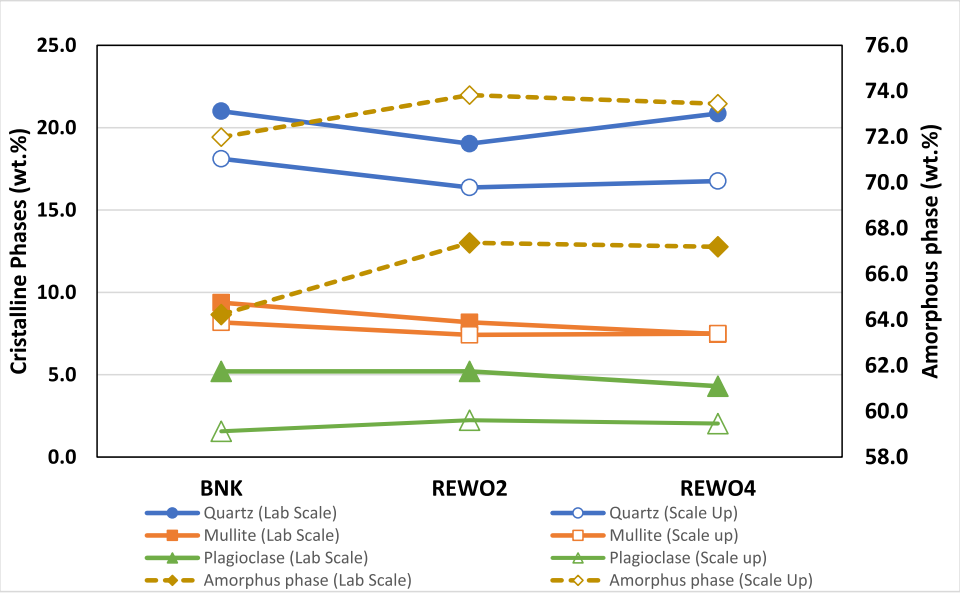

Fig. 5. Quantitative Phase analyses of samples realized in the pilot plant and in the laboratory. All the samples were fired at 1200 °C.

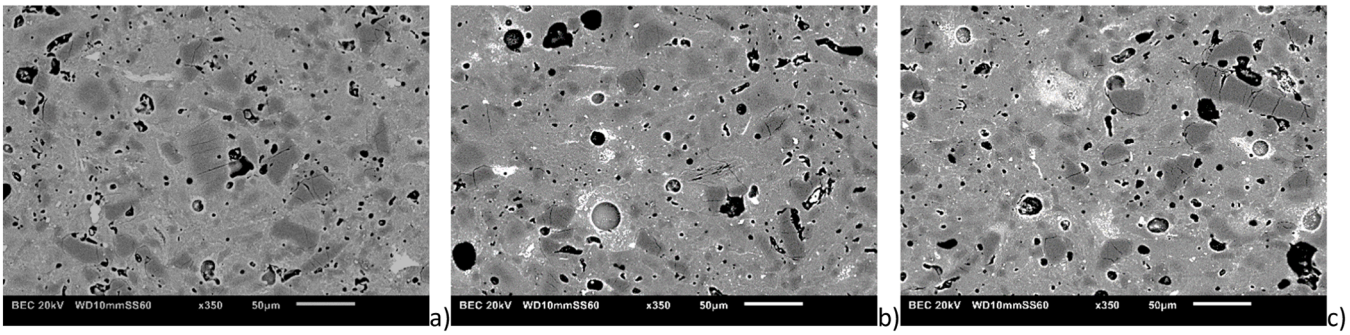

Fig. 6. Backscattered SEM images collected on sample BNK-SU (a), REWO2_SU (b), REWO4_SU(c).

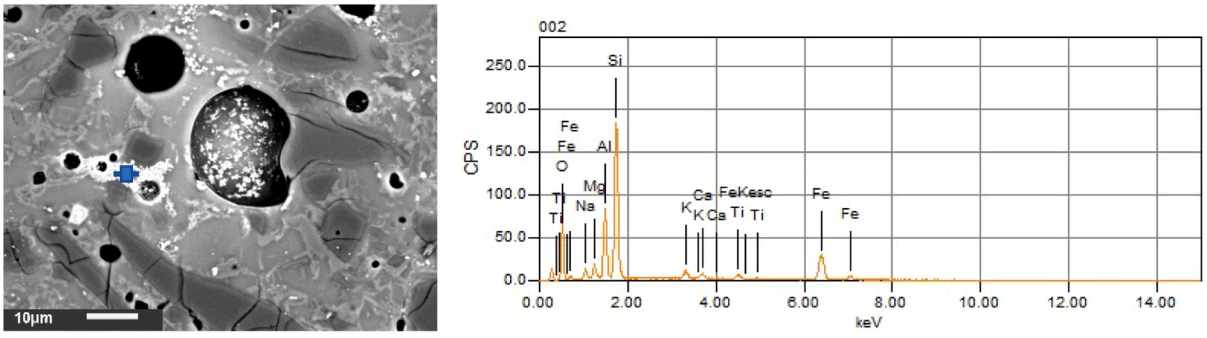

Fig. 7. Backscattered SEM images of a detail of sample REWO4_SU and corresponding EDS spectrum (in blue the analysed area).

resource use, and water use.

To better contextualize the observed differences between the benchmark tile and the formulations containing Re.Wo, two aspects should be considered.

First, although the life cycle inventory of the ceramic tile is predominantly based on reliable primary ceramic industrial data, the MWW inertization process is still represented through industrial-scale design data. As the process has only recently been implemented at industrial scale, its environmental performance may improve over time through more efficient plant operation and optimized oxy-combustion conditions. In this perspective, LCA is useful not only to assess the current environmental profile of the proposed valorisation route, but also to identify the main hotspots for future optimisation. Therefore, despite the uncertainty associated with the observed increase in impacts, the results suggest that further optimization of the MWW inertization process is needed to achieve a scenario in which the incorporation of Re.Wo does not increase, and may potentially reduce, the overall environmental impact of the ceramic tile.

The second aspect concerns the early stage of development of the MWW inertization system itself. Key parameters such as the future

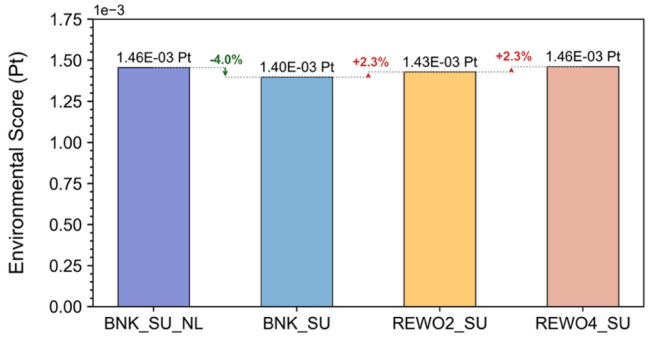

Fig. 8. Midpoint-level environmental single score results (EF 3.1) associated with the life cycle of 1 m^2 of unglazed ceramic tile, with an average thickness of 7.3 mm, an average weight of 17.4 kg/m^2, and a 50-year lifetime, for each formulation considered (BNK_SU_NL, BNK_SU, REWO2_SU, and REWO4_SU).

production volumes, the market value of Re.Wo, and the broader consequences on the conventional management route of mineral wool waste are still uncertain. For this reason, the present assessment should be regarded as prospective and contextual. As these aspects become better defined, complementary modelling approaches, including sensitivity analyses on allocation choices and consequential LCA, may provide a more robust picture of the environmental implications associated with the large-scale implementation of Re.Wo. This would allow consideration of the potential avoided burdens, such as reduced extraction and transport of virgin feldspar (e.g., from Turkey) and the avoidance of landfill for MWW disposal, which does not provide the same level of long-term safety for managing potentially hazardous fibers as inertization.

4. Conclusions

The present work consolidates and extends the research pathway initiated by Arletti et al. [35] and elaborated in Conte et al. [36], providing the demonstration of the feasibility of incorporating inertized mineral wool (Re.Wo) into porcelain stoneware at a pre-industrial scale. By combining localized raw materials, optimized formulations, and pilot-plant processing, this study narrows the gap between laboratory feasibility and pre-industrial validation. The comparison with the previous studies performed by our group [35–37] offers insights into the effect of Re.Wo on technological behaviour, sintering mechanisms, and phase evolution, and highlights the implications for circular economy strategies within the ceramic industry.

A first relevant difference between the present scale-up work and the 2023 laboratory study lies in the raw materials used to formulate the benchmark batch. The previous work adopted Ukrainian ball clays, traditionally employed in porcelain stoneware production, whereas the present study relies on European clays, bentonites, and sands, sourced from Italy and Germany. Despite their different geological provenance, the technological comparison shows that local clays lead to comparable or even improved green strength and densification behaviour. The green flexural strength of the benchmark formulated with local clays (10.2 kg/cm^2) is higher than that reported in the 2023 study (9.3 kg/cm^2), confirming that the shift toward short-distance raw materials does not compromise the mechanical stability of the unfired body. Moreover, the use of local raw materials lowered the optimum firing temperature from 1240 °C to 1200 °C and enhanced the densification efficiency, with a bulk density increased from 2.336 to 2.398 g/cm^3.

The technological evaluation confirms the general trends identified in Arletti et al. [35], namely that modest additions of Re.Wo can be introduced without impairing the compaction or firing behaviour of porcelain stoneware. In the present study, the unfired properties of all batches remain within acceptable industrial ranges, with negligible variations in green shrinkage, springback, and density. This confirms the compatibility of Re.Wo with typical shaping processes used for porcelain stoneware, even when the powders are produced through spray drying rather than laboratory granulation, marking a step forward in technological maturity.

A key result emerging from the scale-up is the identification of 2–4 wt.% Re.Wo as the optimal range for pilot-scale integration. These formulations, in fact, show the most favourable processing window among the investigated compositions within the explored temperature range, with only a modest decrease in bulk density observed at 1220 °C, attributable to the onset of mild bloating. These findings are broadly consistent with the sintering kinetics described here and by Conte et al. [36], where Re.Wo-bearing bodies displayed accelerated liquid-phase sintering above ≈1180 °C due to melt compositional changes.

The gresification curves obtained in the scale-up phase closely match those of the laboratory-scale experiments and mirror the mechanistic evolution described in Conte et al. [36]. Notably, tiles pressed at 350 and 400 kg/cm^2 display comparable densification paths, indicating that Re.Wo does not introduce pressure sensitivity, a potential concern for industrial compaction. The consistency between laboratory and pilot-scale sintering behaviour confirms that the sintering mechanisms identified previously—particularly the competition between melt viscosity, mineral dissolution, and crystalline relic retention— remain broadly consistent at pilot scale.

The successful production of 60 m^2 of tiles for both REWO2 and REWO4 demonstrates that Re.Wo can be processed using standard equipment under pilot-scale conditions, without modification, supporting its pre-industrial feasibility.

Furthermore, the reproducibility of the technological and microstructural trends observed at early TRLs confirms that the incorporation of Re.Wo shows a technologically consistent behaviour within the investigated pilot-scale conditions. This is a major advancement compared with the 2023 study, which validated feasibility only at small scale, and with the 2025 mechanistic work, which focused on fundamental understanding of sintering and microstructure, but not industrial transfer. Although the pilot-scale trial does not yet represent a full industrial demonstration, it provides a meaningful intermediate validation step towards the possible industrial transfer of the process.

The application of the LCA methodology to the formulations tested at TRL6 was intended to provide additional context on the possible environmental implications of Re.Wo incorporation under a prospective large-scale production scenario, also considering the downstream life cycle stages of the finished tile. A first comparison between BNK_SU_NL and the proposed benchmark tile BNK_SU showed that sourcing raw materials locally can lead to a measurable reduction in environmental impacts, thus providing a useful basis for further formulation optimization. The incorporation of Re.Wo at 4 wt.% resulted in a slight increase in environmental impacts, mainly due to a fraction of the burden associated with the highly energy-intensive inertization treatment of MWW. However, the magnitude of these differences remains limited in light of the overall uncertainties of the LCA model, and the results mainly indicate that further improvements in the environmental performance of the inertization step could help reduce this gap. At the same time, as future aspects such as the market availability and production volumes of Re.Wo, as well as its broader influence on conventional MWW management, become clearer, additional modelling approaches, including consequential modelling, may provide a more comprehensive evaluation of the avoided burdens associated with both reduced landfill disposal and reduced consumption of virgin sodic feldspar. In this sense, the LCA does not constitute a major standalone outcome of the present study, but rather identifies the inertization step as the main hotspot for future optimisation and highlights the importance of further improving the environmental performance of the recycling route.

CRediT authorship contribution statement

Sonia Conte: Writing – review & editing, Writing – original draft,

Supervision, Conceptualization. **Francesco Colombo:** Investigation. **Mattia Sisti:** Investigation. **Riccardo Fantini:** Writing – review & editing, Investigation. **Andrea Bresciani:** Methodology, Conceptualization. **Marco Gaddoni:** Methodology, Conceptualization. **Alessandro Francini:** Writing – original draft, Investigation. **Antonella Sola:** Writing – review & editing, Investigation. **Annamaria Ferrari:** Writing – review & editing, Methodology. **Martina Napolitano:** Investigation. **Alessandro F. Gualtieri:** Writing – review & editing, Validation, Methodology. **Rossella Arletti:** Writing – review & editing, Writing – original draft, Supervision, Resources, Project administration, Funding acquisition, Conceptualization.

Declaration of competing interest

The authors declare that they have no known competing financial interests or personal relationships that could have appeared to influence the work reported in this paper.

Acknowledgement

The paper financed by project " FAV4CER:Fibre Vetrose per ceramici green" financed by Ministero dell'Ambiente e della Sicurezza Energetica 2022 CUP E93C23002050006.

Supplementary materials

Supplementary material associated with this article can be found, in the online version, at doi:10.1016/j.rineng.2026.111529.

Data availability

Data will be made available on request.

References

[1] M. Dondi, J. García-Ten, E. Rambaldi, C. Zanelli, M. Vicent-Cabedo, Resource efficiency versus market trends in the ceramic tile industry: effect on the supply chain in Italy and Spain, resources, Conserv. Recycl. 168 (2021) 105271, https://doi.org/10.1016/j.resconrec.2020.105271.

[2] J. García-Ten, M. Dondi, J.V.M.B. Vieira Lisboa, M. Vicent-Cabedo, L. Pérez-Villarejo, E. Rambaldi, C. Zanelli, Critical raw materials in the global high-throughput ceramic industry, Sustainable Mater. Technol. 39 (2024) e00832, https://doi.org/10.1016/j.susmat.2024.e00832.

[3] J. Castellano, V. Sanz, E. Cañas, K. Kayacı, M. Uğur Taşkıran, Ş. Can Genç, E. Sánchez, On the use of Afyon clay in Ukrainian clay-free compositions for porcelain tile manufacture, Boletín de la sociedad española de cerámica y vidrio 63 (2024) 356–367, https://doi.org/10.1016/j.bsecv.2024.05.002.

[4] P. Colombo, G. Brusatin, E. Bernardo, G. Scarinci, Inertization and reuse of waste materials by vitrification and fabrication of glass-based products, Curr. Opin. Solid. State Mater. Sci. 7 (2003) 225–239, https://doi.org/10.1016/j.cossms.2003.08.002.

[5] X. Chen, Y. Tan, H. Yan, J. Shi, J. Wu, B. Ding, A review of cleaner production of glass-ceramics prepared from MSWI fly ash, J. Environ. Manage. 370 (2024) 122855, https://doi.org/10.1016/j.jenvman.2024.122855.

[6] A. Rincón, M. Marangoni, S. Cetin, E. Bernardo, Recycling of inorganic waste in monolithic and cellular glass-based materials for structural and functional applications, J. Chem. Technol. Biotechnol. 91 (2016) 1946–1961, https://doi.org/10.1002/jctb.4982.

[7] W. Fan, B. Liu, X. Luo, J. Yang, B. Guo, S.G. Zhang, Production of glass–ceramics using municipal solid waste incineration fly ash, Rare Met. 38 (2019) 245–251, https://doi.org/10.1007/s12598-017-0976-8.

[8] W. Shang, Z. Peng, Y. Huang, F. Gu, J. Zhang, H. Tang, L. Yang, W. Tian, M. Rao, G. Li, T. Jiang, Production of glass-ceramics from metallurgical slags, J. Clean. Prod. 317 (2021) 128220, https://doi.org/10.1016/j.jclepro.2021.128220.

[9] A.V. Gorokhovsky, G.Y. Yurkov, I.N. Burmistrov, A.F. Villalpando-Reyna, D. V. Kuznetsov, A.A. Gusev, B.B. Khaidarov, Y.V. Konyukhov, O.V. Zakharova, N. V. Kiselev, Glass-ceramic protective coatings based on metallurgical slag, Coatings 13 (2023) 269, https://doi.org/10.3390/coatings13020269.

[10] R.D. Rawlings, J.P. Wu, A.R. Boccaccini, Glass-ceramics: their production from wastes—A review, J. Mater. Sci. 41 (2006) 733–761, https://doi.org/10.1007/s10853-006-6554-3.

[11] R.K. Chinnam, A.A. Francis, J. Will, E. Bernardo, A.R. Boccaccini, Review, functional glasses and glass-ceramics derived from iron rich waste and combination of industrial residues, J. Non. Cryst. Solids. 365 (2013) 63–74, https://doi.org/10.1016/j.jnoncrysol.2012.12.006.

[12] E. Bernardo, R. Cedro, M. Florean, S. Hreglich, Reutilization and stabilization of wastes by the production of glass foams, Ceram. Int. 33 (2007) 963–968, https://doi.org/10.1016/j.ceramint.2006.02.010.

[13] M.B. Almendro-Candel, M.M. Jordán Vidal, Glasses, frits and glass-ceramics: processes and uses in the context of circular economy and waste vitrification, Coatings 14 (2024) 346, https://doi.org/10.3390/coatings14030346.

[14] S. Conte, C. Zanelli, M. Ardit, G. Cruciani, M. Dondi, Predicting viscosity and surface tension at high temperature of porcelain stoneware bodies: a methodological approach, Materials 11 (2018) 2475, https://doi.org/10.3390/ma11122475.

[15] S. Conte, C. Zanelli, M. Ardit, G. Cruciani, M. Dondi, Phase evolution during reactive sintering by viscous flow: disclosing the inner workings in porcelain stoneware firing, J. Eur. Ceram. Soc. 40 (2020) 1738–1752, https://doi.org/10.1016/j.jeurceramsoc.2019.12.030, a.

[16] S. Conte, C. Molinari, M. Ardit, G. Cruciani, M. Dondi, C. Zanelli, Porcelain versus Porcelain stoneware: so close, so different. Sintering kinetics, phase evolution, and vitrification paths, Materials 16 (2023) 171, https://doi.org/10.3390/ma16010171.

[17] F. Matteucci, M. Dondi, G. Guarini, Effect of soda-lime glass on sintering and technological properties of porcelain stoneware tiles, Ceram. Int. 28 (8) (2002) 873–880, https://doi.org/10.1016/S0272-8842(02)00067-6.

[18] C. Carbonchi, P. Danasino, R. Lorici, R. Riveriti, E. Castelli, Impiego di fondenti additivati con vetro in un impasto da gres porcellanato, Ceramica Informazione 426 (2003) 580–587. http://mineraliindustriali.serverand.it/wp-content/uploads/2016/04/C7.pdf.

[19] E. Rambaldi, A. Tucci, L. Esposito, Glass recycling in porcelain stoneware tiles: firing behaviour, Ceram. Forum Int. cfi-Ber. DKG 81 (3) (2004) E32–E36. https://www.researchgate.net/publication/292135293_Glass_Recycling_in_Porcelain_Stoneware_Tiles_Firing_Behaviour.

[20] E. Rambaldi, W.M. Carty, A. Tucci, L. Esposito, Using waste glass as a partial flux substitution and pyroplastic deformation of a porcelain stoneware tile body, Ceram. Int. 33 (5) (2007) 727–733, https://doi.org/10.1016/j.ceramint.2005.12.010.

[21] A. Tucci, L. Esposito, E. Rastelli, C. Palmonari, E. Rambaldi, Use of soda-lime scrap-glass as a fluxing agent in a porcelain stoneware tile mix, J. Eur. Ceram. Soc. 24 (1) (2004) 83–92, https://doi.org/10.1016/S0955-2219(03)00121-3.

[22] A. Tucci, E. Rambaldi, L. Esposito, Use of scrap glass as raw material for porcelain stoneware tiles, Adv. Appl. Ceram. 105 (1) (2006) 40–45, https://doi.org/10.1179/174367606X81713.

[23] I.M. Bakr, Effect of waste glass and zircon on ceramic properties and microstructure of porcelain tiles, Adv. Appl. Ceram. 104 (5) (2005) 243–248, https://doi.org/10.1179/174367605X52031.

[24] Y. Pontikes, A. Christogerou, G.N. Angelopoulos, E. Rambaldi, L. Esposito, A. Tucci, Use of scrap soda–lime–silica glass in traditional ceramics, Glass Technol. 46 (2) (2005) 200–206. https://www.researchgate.net/publication/233703422_Use_of_scrap_sodalimesilica_glass_in_traditional_ceramics.

[25] T. Tarvornpanich, G.P. Souza, W.E. Lee, Microstructural evolution on firing soda–lime–silica glass fluxed whitewares, J. Am. Ceram. Soc. 88 (5) (2005) 1302–1308, https://doi.org/10.1111/j.1551-2916.2005.00292.x.

[26] S. Mustafi, M. Ahsan, A.H. Dewan, S. Ahmed, N. Khatun, N. Absar, Effect of waste glass powder on physico-mechanical properties of ceramic tiles, Bangladesh J. Sci. Res. 24 (2) (2012) 169–180, https://doi.org/10.3329/bjsr.v24i2.10775.

[27] K.O. Ajanaku, M. Pal, S.K. Das, Differences in vitrification behaviour of flint and opaque scrap glass containing porcelainized stoneware body, Ceramic Forum International, cfi/Ber, DKG 92 (3) (2015) 31–34. https://www.researchgate.net/publication/317204885_Differences_in_vitrification_behaviour_of_flint_and_opaque_scrap_glass_containing_porcelainized_stoneware_body.

[28] M. Raimondo, C. Zanelli, F. Matteucci, G. Guarini, M. Dondi, J.A. Labrincha, Effect of waste glass (TV/PC cathodic tube and screen) on technological properties and sintering behaviour of porcelain stoneware tiles, Ceram. Int. 33 (4) (2006) 615–623, https://doi.org/10.1016/j.ceramint.2005.11.012.

[29] N.M.F. Andreola, L. Barbieri, E. Karamanova, I. Lancellotti, M. Pelino, Recycling of CRT panel glass as fluxing agent in the porcelain stoneware tile production, Ceram. Int. 34 (5) (2008) 1289–1295, https://doi.org/10.1016/j.ceramint.2007.03.013.

[30] K. Kim, K. Kim, J. Hwang, Characterization of ceramic tiles containing LCD waste glass, Ceram. Int. 42 (6) (2016) 7626–7631, https://doi.org/10.1016/j.ceramint.2016.01.172.

[31] E. Bernardo, A. Dattoli, E. Bonomo, L. Esposito, E. Rambaldi, A. Tucci, Application of an industrial waste glass in "glass–ceramic stoneware, Int. J. Appl. Ceram. Technol. 8 (5) (2011) 1153–1162, https://doi.org/10.1111/j.1744-7402.2010.02550.x.

[32] E. Bernardo, L. Esposito, E. Rambaldi, A. Tucci, S. Hreglich, Recycle of waste glass into "glass–Ceramic stoneware, J. Am. Ceram. Soc. 91 (7) (2008) 2156–2162, https://doi.org/10.1111/j.1551-2916.2008.02460.x.

[33] E. Bernardo, L. Esposito, S. Hreglich, E. Rambaldi, G. Timellini, A. Tucci, Tailored waste based glasses as secondary raw materials for porcelain stoneware, Adv. Appl. Ceram. 107 (6) (2008) 322–328, https://doi.org/10.1179/174367508X289460.

[34] C. Zanelli, S. Conte, C. Molinari, S. Soldati, M. Dondi, Waste recycling in ceramic tiles: a technological outlook, Resour. Conserv. Recycl. 168 (2021) 105289, https://doi.org/10.1016/j.resconrec.2020.105289.

[35] R. Arletti, S. Conte, C. Zanelli, M. De Iuliis, D. Di Giuseppe, V. Scognamiglio, D. Malferrari, M. Dondi, A.F. Gualtieri, Recycling the product of thermal inertization of man-made vitreous fibres for the manufacture of stoneware tiles, Waste Biomass Valor. 14 (2023) 1721–1736, https://doi.org/10.1007/s12649-022-01959-8.

[36] S. Conte, R. Fantini, R. Arletti, C. Molinari, M. Dondi, C. Zanelli, A.F. Gualtieri, Sintering mechanisms, phase transformations and microstructure of porcelain stoneware containing thermally inertized man-made vitreous fibres, J. Eur. Ceram. Soc. 45 (2025) 117230, https://doi.org/10.1016/j.jeurceramsoc.2025.117230 a.
[37] M. Sisti, D. Guidetti, F. Altimari, F. Andreola, L. Barbieri, I. Lancellotti, L. Casini, F. Colombo, R. Arletti, R. Fantini, A.F. Gualtieri, Sustainable glazes for ceramic tiles: exploiting inertized man-made vitreous fibres waste as a resource, Ceram. Int. 51 (2025) 4195–4205, https://doi.org/10.1016/j.ceramint.2024.11.396.
[38] S. Sarner, O. Guillon, A perspective on ceramic recycling, J. Eur. Ceram. Soc. 45 (2025) 117511, https://doi.org/10.1016/j.jeurceramsoc.2025.117511.
[39] A.F. Gualtieri, G.D. Gatta, A. Arletti, G. Artioli, P. Ballirano, G. Cruciani, Quantitative phase analysis using the Rietveld method: towards a procedure for checking the reliability and quality of the results, Periodico di Mineralogia 88 (2) (2019), https://doi.org/10.2451/2019PM870.
[40] N. Döbelin, R. Kleeberg, Profex: a graphical user interface for the Rietveld refinement program BGMN, J. Appl. Crystallogr. 48 (2015) 1573–1580, https://doi.org/10.1107/S1600576715014685.
[41] Larson A.C., Dreele R.B., General structure Analysis System – GSAS/EXPGUI, vol. 48 (2000) p. 86.
[42] B.H. Toby, EXPGUI, a graphical user interface for GSAS, J. Appl. Crystallogr. 34 (2001) 210–213, https://doi.org/10.1107/S0021889801002242.
[43] F. Andreola, L. Barbieri, F. Bondioli, I. Lancellotti, P. Miselli, A.M. Ferrari, Recycling of screen glass into new traditional ceramic materials: recycling of screen glass in ceramics, Int. J. Appl. Ceram. Technol. 7 (2010) 909–917, https://doi.org/10.1111/j.1744-7402.2009.02378.x.
[44] S. Chitwaree, J. Tiansuwan, N. Thavarungkul, L. Punsukumtana, Energy saving in sintering of porcelain stoneware tile manufacturing by using recycled glass and pottery stone as substitute materials, Case Stud. Therm. Eng. 11 (2018) 81–88, https://doi.org/10.1016/j.csite.2018.01.002.
[45] S. Conte, C. Zanelli, C. Molinari, G. Guarini, M. Dondi, Glassy wastes as feldspar substitutes in porcelain stoneware tiles: thermal behaviour and effect on sintering process, Mater. Chem. Phys. 256 (2020) 123613, https://doi.org/10.1016/j.matchemphys.2020.123613 b.
[46] A.P. Luz, S. Ribeiro, Use of glass waste as a raw material in porcelain stoneware tile mixtures, Ceram. Int. 33 (2007) 761–765, https://doi.org/10.1016/j.ceramint.2006.01.001.
[47] N. Marinoni, D. D'Alessio, V. Diella, A. Pavese, F. Francescon, Effects of soda–lime–silica waste glass on mullite formation kinetics and micro-structures development in vitreous ceramics, J. Environ. Manage. 124 (2013) 100–107, https://doi.org/10.1016/j.jenvman.2013.02.048.
[48] International Organization for Standardization, ISO 14040:2006 environmental management — Life cycle assessment — Principles and framework, a, https://www.iso.org/standard/37456.html, 2006.
[49] International Organization for Standardization, ISO 14044:2006 environmental management — Life cycle assessment — Requirements and guidelines, b, https://www.iso.org/standard/38498.html, 2006.
[50] A.M. Ferrari, L. Volpi, D. Settembre-Blundo, F.E. García-Muiña, Dynamic life cycle assessment (LCA) integrating life cycle inventory (LCI) and enterprise resource planning (ERP) in an industry 4.0 environment, J. Clean. Prod. 286 (2021) 125314, https://doi.org/10.1016/j.jclepro.2020.125314.
[51] I. Zanatto, A.F. Gualtieri, Apparato per il trattamento di rifiuti contenenti lana minerale, Italian Patent N (2022), 102021000002246, https://patentimages.storage.googleapis.com/4a/47/94/7ec09aed05fcd0/IT202100002246A1.pdf.
[52] B.P. Weidema, C. Bauer, R. Hischier, C. Mutel, T. Nemecek, J. Reinhard, O. C. Vadenbo, G. Wernet, Overview and methodology - data quality guideline for the ecoinvent database version 3, Ecoinvent Report, in: Swiss Centre for Life Cycle Inventories, 3, The ecoinvent Centre, St. Gallen, 2013. https://vbn.aau.dk/ws/files/176769045/overview_and_methodology.pdf.
[53] G. Wernet, C. Bauer, B. Steubing, J. Reinhard, E. Moreno-Ruiz, B. Weidema, The ecoinvent database version 3 (part I): overview and methodology, Int. J. Life Cycle Assess. 21 (2016) 1218–1230, https://doi.org/10.1007/s11367-016-1087-8.
[54] B.V. SimaPro, SimaPro 9.6.0.1 [Software], https://support.simapro.com/en/articles/504757-release-notes-simapro-desktop#h_d7a61d06fe, 2024 (accessed 10/4/2026).
[55] M. Pini, S. Scarpellini, R. Rosa, P. Neri, A.F. Gualtieri, A.M. Ferrari, Management of asbestos containing materials: a detailed LCA comparison of different scenarios comprising first time asbestos characterization factor proposal, Environ. Sci. Technol. 55 (2021) 12672–12682, https://doi.org/10.1021/acs.est.1c02410.
[56] European Commission, Joint Research Centre, Updated Characterisation and Normalisation Factors For the Environmental Footprint 3.1 Method, Publications Office, LU, 2023, https://doi.org/10.2760/798894 online.
[57] B.V. SimaPro, SimaPro database manual - methods library. https://support.simapro.com/en/articles/504752-simapro-methods-manual, 2026 accessed 10/4/2026.
[58] E.N. CEN, 15804:2012+A2:2019 - Sustainability of construction works, environmental product declarations, core rules for the product category of construction products. https://nmfv.dk/wp-content/uploads/2024/01/EN-15804-A2.pdf, 2019.
[59] European Commission, Eds., in: S. Sala, A.K. Cerutti, R. Pant (Eds.), Development of a Weighting Approach For the Environmental Footprint, Publications Office, Luxembourg, 2018 https://doi.org/10.2760/446145.
[60] M. Darolt, M. Cargnin, A. Peterson, Noni De Jr., Additional high-energy milling to enhance the performance of porcelain stoneware manufacturing, Int. J. Appl. Ceram. 17 (2020) 1742–1751, https://doi.org/10.1111/ijac.13478.
[61] J.L. Amorós, M.J. Orts, J. García-Ten, A. Gozalbo, E. Sánchez, Effect of the green porous texture on porcelain tile properties, J. Eur. Ceram. Soc. 27 (2007) 2295–2301, https://doi.org/10.1016/j.jeurceramsoc.2006.07.005.
[62] S. Conte, C. Molinari, M. Dondi, G. Guarini, C. Zanelli, Effect of milling and compaction of porcelain stoneware tiles, Ceram. Int. 50 (2024) 25228–25240, https://doi.org/10.1016/j.ceramint.2024.04.253.
[63] S. Conte, C. Molinari, M. Ardit, D. Giordano, M. Dondi, C. Zanelli, Vitrification paths in porcelain stoneware: dependence on bulk chemical composition and effect on sintering behaviour, Ceram. Int. 51 (2025) 36777–36789, https://doi.org/10.1016/j.ceramint.2025.05.388, b.
[64] R. Fantini, S. Conte, C. Molinari, C. Zanelli, M. Dondi, M. Bernini, A.F. Gualtieri, R. Arletti, Valorizing carbonate-rich mining waste in porcelain stoneware production, Ceram. Int. 52 (2026) 735–747, https://doi.org/10.1016/j.ceramint.2025.11.373.
[65] S.R. Bragança, C.P. Bergmann, Porcelain casting slips formulated with waste glass, Int. J. Appl. Ceram. Technol. 6 (2) (2009) 264–269, https://doi.org/10.1111/j.1744-7402.2008.02266.x.
[66] M.G. Moshnyakov, V.Z. Abdrakhimov, Investigations of the black core and swelling in firing porcelain stoneware, Glass Ceram. 76 (2019) 270–273, https://doi.org/10.1007/s10717-019-00181-8.
[67] M. Engels, S. Link, Bubble control in ceramic glazes. https://www.researchgate.net/publication/292879264_Bubble_control_in_ceramic_glazes_Part_1, 2006.
[68] J.M. Pérez, M. Romero, Microstructure and technological properties of porcelain stoneware tiles moulded at different pressures and thicknesses, Ceram. Int. 40 (2014) 1365–1377, https://doi.org/10.1016/j.ceramint.2013.07.018.
[69] O. Jolliet, M. Saadé-Sbeih, S. Shaked, A. Jolliet, P. Crettaz, Environmental Life Cycle Assessment, CRC Press, Boca Raton, 2016, https://doi.org/10.1201/b19138.